ELECTRON PARAMAGNETIC DOUBLE RESONANCE AND SPIN RELAXATION OF ORGANIC FREE RADICALS IN SOLUTION

Hideo Shikata

1993

Laboratory of Chemistry
Faculty of General Education
Ehime University

Acknowledgement

The present work is the collection of the studies, which have been carried out both at Ehime University and at Osaka University. Through all these studies, I was always guided by Prof. K. Ishizu of Ehime University and Prof. K. Kuwata of Osaka University. It was the first ENDOR experiment for me, when I had observed the ENDOR enhancement of dicyanobiphenyl radical anions under leading by Prof. Ishizu. Surprisingly remarkable optimum temperature observed at that time have just urged me to start the present study. Under the guidance by Prof. Kuwata, I could learn and master relaxation theories and the experimental techniques for measuring ELDOR reduction at Osaka University. Also it was during the discussion with him as well as with his colleagues, Dr. Doi and others, that I conceived an idea to calculate the fractional ENDOR enhancement for a multi-level system. It is my pleasure to acknowledge sincerely their stimulating encouragement and kind instruction on both theoretical and experimental issue of the subject.

I am grateful to Prof. H. Takaki and Prof. Y. Deguchi whose guidance in my undergraduate and graduate course at Kyoto University is the basis of the present work. Especially, translation to Japanese of the book by Prof. Pake, "Paramagnetic Resonance", by our ESR group at those times, brought straight-forwardly on an idea of the present theory for double resonance, based on spin population number method.

I am gratefully in debt to experimental performance as well as exacting criticism by Prof. K. Mukai and Assist. Prof. K.Tajima of Ehime University. I also wish to thank Mr. M. Ohnishi and Mr. Y. Nishimoto for their skilful experimental assistances.

Contents

1.1 Electron Paramagnetic Double Resonance

1.1.1 Definition and Origin

The resonance spectroscopy is a method to observe resonated interaction between molecules and coherent radiations. In double resonance experiments, two modes of the coherent fields are simultaneously irradiated, one for exciting and another for observing; the effect of the transition induced by the exciting mode radiation is monitored by another transition induced by the observing mode radiation.

The double resonance technique was historically originated by Block[1] at an early stage of the study of proton nuclear magnetic resonance (**NMR**). The method was developed by Royden[2] and was treated by Bloom and Shoolery[3] from the experimental and theoretical viewpoint. Their method of double irradiation by two radio frequency (rf) fields is now called the spin decoupling; It is now practically indispensable to simplify high resolution NMR spectra as well as to get detailed information as for couplings among nuclear species. On the other hand, the population rearrangement of nuclear spins in consequence of saturating electron spin transitions was proposed by Overhauser.[4] The effect was experimentally observed by Carter and Slichter,[5] shortly thereafter. The Overhauser effect, the "Underhauser" effect,[6] and so called the solid state effect[7] are genetically named as dynamic

---

1 F. Block, *Phys. Rev.*, **93**, 944 (1954).

2 V. Royden, *Phys. Rev.*, **96**, 543 (1954).

3 A. L. Bloom and J. N. Shoolery, *Phys. Rev.*, **97**, 1261 (1955).

4 A. W. Overhauser, *Phys. Rev.*, **92**, 411 (1953).

5 T. R. Carter and C. P. Slichter, *Phys. Rev.*, **102**, 975 (1956).

6 A. Abragam, *Phys. Rev.*, **98**, 1729 (1955).

nuclear polarization[*1] or nuclear electron double resonance (**NEDOR**). The induced emission from a system characterized by the negative spin temperature or the population inversion, which results from the strong microwave (**mw**) irradiation, was observed by Purcell and Pound[8] using the NMR method. Their idea came to fruition by Towns and coworkers as the ammonia MASER[9] or the ruby MASER.[10] The latter utilizes the population inversion between the Zeeman levels of the paramagnetic impurities, so it conceptually may associates with the electron electron double resonance.

It should be noted here that historically, the most practical and convenient method to describe the double resonance phenomena, mentioned above, have been to solve the rate equations governing the population numbers on the various energy levels, which were first established by Lloyde and Pake.[11] For instance, three-level solid state MASER was first proposed by Bloembergen[12] by applying this method, and was observed thereafter by Scovil *et al.*[13]

In electron paramagnetic resonance (**EPR**) spectroscopy, the term,

---

*1 Today this term includes also the chemically induced dynamic nuclear polarization.

7 A. Abragam and W. G. Procter, *Comp. Rend.*, **246**, 2253 (1958).

8 E. M. Purcell and R. V. Pound, *Phys. Rev.*, **81**, 279 (1951).

9 J. P. Gorden, H. J. Zeiger, and C. H. Towns, *Phys. Rev.*, **95**, 282 (1954).

10 J. A. Giormaine, L. E. Alsop, C. H. Mayer, and C. H. Towns, *Proc. IRE*, **47**, 1958 (1959).

11 J. P. Lloyde and G. E. Pake, *Phys. Rev.*, **94**, 579 (1954).

12 N. Bloembergen, *Phys. Rev.*, **104**, 324 (1956).

13 H. E. Scovil, G. Feher, and H. Seidel, *Phys. Rev.*, **105**, 7 (1957).

14 G. Feher, *Phys. Rev.*, **103**, 834 (1956).

"electron paramagnetic double resonance (**EPDR**)", is referred to the experimental methods in which the effect on EPR is observed, during simultaneous irradiation of another rf field or mw field.*2 The former is called electron nuclear double resonance (**ENDOR**), whereas the latter is called electron electron double resonance (**ELDOR**), depending on whether the NMR or the EPR transition is induced by the second exciting magnetic field, during monitoring EPR transition. ENDOR and ELDOR are, in principle, the counterpart of dynamic nuclear polarization and spin decoupling, respectively, in NMR spectroscopy.

The first successful ENDOR experiment was carried out by Feher[14] in 1956, concerning with phosphorus doped in silicon. The technique was subsequently applied to investigations on solid state substances, for instances, semiconductors,[15,16] color centers in alkali halides,[17,18] and trapped paramagnetic ions[19] or radicals[20,21] in single crystals or powders.[22]

The ENDOR or ELDOR observation for radicals in liquid phase requires

---

*2 In the present study, the rf field is named to the electromagnetic field of frequency smaller than 500 MHz, whereas the mw field to that of the order of 10GHz.

15 G. Feher, C. S. Fuller, and E. A. Gere, *Phys. Rev.*, **107**, 1462 (1957); G. Feher, *ibid.*, **114**, 1245 (1959); E. C. McIrvine, J. Lambe, and N. Laurance, *ibid.*, **136**, A467 (1964).

16 G. Feher, *Phys. Rev.*, **114**, 1219 (1959).

17 G. Feher, *Phys. Rev.*, **105**, 1122 (1957); W. C. Holton, H. Blum, and C. P. Slichter, *Phys. Rev. Lett.*, **5**, 197 (1960); W. C. Holton and H. Blum, *Phys. Rev.*, **125**, 89 (1962); W. T. Doyle, *ibid.*, **126**, 1421 (1962).

18 H. Seidel, *Z. Physik*, **165**, 218 (1961).

19 R. W. Terhune, J. Lambe, G. Makhov, and L. G. Gross, *Phys. Rev. Lett.*, **4**, 234 (1960). G. Feher, C. S. Fuller, and E. A. Gere, *Phys. Rev.*, **107**, 1462 (1957); G. Feher, *ibid.*, **114**,

much stronger rf power or mw power, effectively irradiated on samples, than in solid phase. So it was not until 1964 that Hyde and Maki[23] first succeeded in observing the ENDOR enhancement of the galvinoxyl radical in toluene solution. Also, in 1968, after eight years, since the first observation of ELDOR reduction for nitrogen in diamond by Solokin *et al.*,[24] Hyde, Chien, and Freed[25] first succeeded in observing the liquid phase ELDOR reduction of the galvinoxyl and some nitroxide radicals, with an elaborated microwave techniques. Since then, the utility of both ENDOR and ELDOR has been extensively recognized and now more than hundred investigations on solid and liquid phase substances have been reported in literatures.[26,27,28]

1245 (1959); E. C. McIrvine, J. Lambe, and N. Laurance, *ibid.*, **136**, A467 (1964).

20 J. Lambe, N. Laurance, E. C. McIrvine, and R. W. Terhune, *Phys. Rev.*, **122**, 1161 (1961); R. J. Cook and D. H. Wiffen, *Proc. Loy. Soc.*, **84**, 845 (1964); H. Muto, K. Nunome, and M. Iwasaki, *J. Chem. Phys.*, **61**, 1075 (1974).

21 R. J. Cook and D. H. Whiffen, *Proc. Loy. Soc.*, **A295**, 99 (1966).

22 D. S. Leniart, J. S. Hyde, and J. C. Vedrine, *J. Phys. Chem.*, **76**, 2079 (1972).

23 J. S. Hyde and A. H. Maki, *J. Chem. Phys.*, **40**, 3117 (1964).

24 P. P. Solokin, G. J. Lasher, and I. L. Gelles, *Phys. Rev.*, **118**, 939 (1960),

25 J. S. Hyde, J. C. W. Chien, and J. H. Freed, *J. Chem. Phys.*, **48**, 4211 (1968).

26 A. L. Kwiram, *Ann. Rev. Phys. Chem.*,**22**, 133 (1971); N. M. Atherton, "Electron Spin Resonance", John Wiley & Sons, New York (1973).

27 L. Kevan and L. D. Kispert, "Electron Spin Double Resonance Spectroscopy", John Wiley & Sons, New York (1976).

Other form of multiple EPR has been also reported in literature. Movius *et al*[29] succeeded to observe electron nuclear nuclear triple resonance (**TRIPLE**) for liquid phase radicals. Another combination for multiple resonance is the optical detection of EPR,[30] ENDOR,[31] and ELDOR[32] of the triplet states (**ODMR**); The rate of radiative decay differs appreciably among three sublevels of the triplets at liquid He temperatures. This results in the change of the phosphorescence intensity when mw and/or rf fields are resonated among three levels. Such techniques have been proven quite useful for the study of the electronic structure and the energy transfer of the triplet state molecules.

Double resonance techniques are not the monopoly of magnetic resonance spectroscopies. With progress of LASER techniques, they have become commonly utilized in recent optical spectroscopies. Infrared (IR) double resonance,[33] IR mw double resonance[34] and mw double resonance[35] are the samples. These methods are applied as a powerful tool to the

---

28 H. Kureck, B. Kirste, and W. Lubitz, "Electron Nuclear Double Resonance Spectroscopy of Radicals in Solution", VCH Publisher Ltd. (1988).

29 K. P. Dinse, R. Biehl, and K. Movius, *J. Chem Phys.*, **61**, 4335 (1974).

30 J. Brossel and F. Bitter, *Phys. Rev.*, **86**, 308 (1952); S. Geschwind, R. J. Collins, and A. L. Shawlow, *Phys. Rev. Lett.*, **3**, 545 (1959); J. Schmidt, I. A. M. Hesselman, M. S. de Groot, and J. H. van der Waals, *Chem. Phys. Lett.*, **1**, 434 (1967).

31 C. B. Harris, D. S. Timti, M. A. El-Sayed, and A. H. Maki, *Chem. Phys. Lett.*, **4**, 409 (1969); I. Y. Chan, J. Schmidt, and J. H. van der Waals, *ibid.*, **4**, 269 (1969).

32 T. S. Kuan, D. S. Tinti, and M. A. El-Sayed, *Chem. Phys. Lett.*, **4**, 507 (1970).

33 C. K. Phodes, M. J. Kelly, and A. Javan, *J. Chem. Phys.*, **48**, 5730 (1968).

detailed examination of the energy transfer processes, such as T-V, V-T, and V-R processes of gaseous state molecules.

1.1.2 General Features and Utility of Electron Paramagnetic Double Resonance

The principal advantage of the resonance experiments, compared with the non-resonance one, should be the possible observation of highly selective transitions. This enables the measurement of sharp absorption lines with prominent sensitivity. Above such prominence, the magnetic resonance experiments are favorable in that they can extract the "purified" information, that is, only the information connected directly or indirectly with magnetic interactions from among various miscellaneous molecular interactions. Thus, kinds of magnetic interactions can be well identified and their magnitude can be quantum-mechanically calculated with required precision.

The general feature of EPDR lies on the same line as that of the single resonance, mentioned above. But it consists in much more emphasized fashion. In EPDR experiments, two independent and coherent mw and/or rf fields are simultaneously irradiated so that one can observe, at least indirectly, transitions more specified and more subtly controlled, than in single resonance one. This feature divides the utility of EPDR largely into two; more sensitive and accurate measurement of the resonance

---

[34] T. Shimizu and T. Oka, *Phys. Rev.*, **A2**, 1177 (1970); J. M. Levy, J. H. S. Wang, S. G. Kukoluch, and J. I. Steinfeld, *Phys. Rev. Lett.*, **29**, 395 (1972).

[35] A. Battaglia, A. Gozzini, and E. Polacco, *Nuovo Cim.*, **2**, 1076 (1959).

frequencies, and more detailed analysis of the relaxation processes. An alternative classification may be acquisition of precise information about the "statical" and "dynamical" structure of the molecular system. In the following, these are discussed mainly focusing our attention to those of liquid phase ENDOR and ELDOR.

a) Study of statical structure

The characteristic of EPR spectra for radicals in liquid phase, compared with other phase, is their hyperfine structure, and thus the direct observable of EPR experiments is obtained as the hyperfine splitting (**hfs**) constants as well as the g-values. From the hfs constants we obtain the experimental value of unpaired electron densities by use of the McConell relation,[36]

$$a_H = Q^H_{CH} \rho_C \qquad (1.1.1)$$

or its derivative,[37] where a_H is the hfs constant of a proton, ρ_C is the unpaired electron density on a carbon atom to which the observing proton is bonded, and Q^H_{CH} is the $\sigma - \pi$ polarization constant which takes a value typically in the range, 60 - 90 MHz. Comparing the experimental spin density of each carbon atom with the result of the molecular orbital calculation such as of the Huckel-McLachlan MO method,[38] one can assigne the kind and the position in the molecule with the number of equivalent nuclei. Also, one can get information as for the electronic structure of the

---

36 H. M. McConell, *J. Chem. Phys.*, **24**, 764 (1956).

37 M. Karplus and G. K. Fraenkel, *J. Chem. Phys.*, **35**, 1312 (1961).

38 A. D. MacLachlan, *Mol. Phys.*, **3**, 233 (1960).

radical, and further in some case, as for its molecular conformation. Obtaining accurate hfs constants will enable more accurate description. For several reasons, ENDOR and ELDOR offer a quite powerful tool for this purpose.

First, apparent enhancement of the sensitivity is often encountered: In ENDOR, nuclear spin transitions are indirectly monitored through electron spin transitions. Therefore one can expect for ENDOR enhancement $\mu_e/\mu_n \fallingdotseq 103$ times higher sensitivity than for single NMR, where μ_e and μ_n are the electron- and the nuclear magnetic moments, respectively.

Second, ENDOR and ELDOR give, in general, much simpler spectra than those of EPR: [39,25] The EPR spectra of radicals which have several sets of equivalent protons and other nuclei are often obscured due to superposition of the component lines. Furthermore each line should be often considered to be the Gaussian envelope of a set of small unresolved hfs's. Among many spin packets, responsible for such "inhomogeneous broadening", only a limited number of spin packets can be desaturated in ENDOR, or saturated in ELDOR, due to second exciting magnetic field, so that, as Seidel had already indicated,[18] rf irradiation brings on a shortening of the effective T_{1e}, which results in desaturation of the previously saturated EPR line so as to increase the EPR intensity. Thus, the ENDOR enhancement is calculated as principle, much sharper and much resolved spectra than EPR does: The line width of ENDOR spectra must be essentially that of one nuclear spin packet (See Eq. (2.3.82)); usually it lies

---

*3 (next page) It is noted, however, that the line width of a nuclear spin packet in a radical is considerably larger than that in a diamagnetic molecule, because of coupling of nuclei with unpaired electron spins.

39 J. S. Hyde, *J. Chem. Phys.*, **43**, 1806 (1965).

in the region, 10 - 50 kHz,[*3] which are much narrower than 1 - 5 MHz of inhomogeneously broadened EPR line widths.

Many radicals in liquid phase have been observed taking advantage of these features of EPDR. Many are the negative ions such as semiquinones,[39,40,41] aromatic hydrocarbon radicals reduced by alkali metals or alkaline earth metals.[42-45] Many are the neutral radicals such as triphenyl methyls,[39,46-48] phenoxyls,[49-52,53] nitroxides,[54] hydrazyls,[55] cyclopentadienyls,[56] and verdazyls.[57] Few are the positive ions.[39,58]

---

40 M. R. Das, H. D. Connor, D. S. Leniart, and J. H. Freed, *J. Amer. Chem. Soc.*, **92**, 2258 (1970); R. D. Allendoerfer and R. J. Papetz, *ibid.*, **92**, 6971 (1970).

41 Y. Kotake and K. Kuwata, *Bull. Chem. Soc. Jpn.*,**47**, 45 (1974).

42 A. Lagendijk, N. F. Tromp, M. Glabeek, and J. D. W van Voorst, *Chem. Phys. Lett.*, **6**, 152 (1970); R. Biehl, K. P. Dinse, and K. Mobius, *ibid.*, **10**, 605 (1971).

43 N. M. Atherton and B. Day, *J. Chem. Soc. Faraday Trans., II*, **69**, 1801 (1979); K. Ishizu, F. Nemoto, K. Mukai, M. Kohno, and H. Hasegawa, *Bull. Chem. Soc. Jpn.*, **48**, 1635 (1975); F. Nemoto, F. Shimoda, and K. Ishizu, *ibid.*, **48**, 2627 (1975).

44 H. van Willigen, M. Plato, R. Biehl, K. P. Dinse, and K. Mobius, *Mol. Phys.*, **26**, 793 (1973).

45 K. Ishizu, N. Ohnishi, and H. Shikata, *Bull. Chem. Soc. Jpn.*, **50**, 76 (1973).

46 J. S. Hyde, G. H. List, and L. F. G. Eriksson, *J. Phys. Soc.*, **72**, 4269 (1958); A. H. Maki, R. D. Allendoefer, J. C. Danner, and R. T. Keys, *J. Amer. Chem. Soc.*, **90**, 4225 (1968); J. S. Hyde, R. Breslow, and C. deBoer, *ibid.*, **88**, 4763 (1966).

47 R. D. Allendoefer and A. H. Maki, *ibid.*, **91**, 1088 (1969).

48 L. D. Kispert, J. S. Hyde, C. deBoer, D. Lafolltte, and R. Breslow, *J. Phys. Chem.*, **72**, 4276 (1968).

49 J. S. Hyde, *J. Phys. Chem.*, **71**, 68 (1967).

50 R. D. Allendoefer and A. H. Maki, *J. Mag. Res.*, **3**, 396 (1970).

51 N. M. Atherton and B. Day, *Mol. Phys.*, **27**, 145 (1974).

By ENDOR even very small hfs's which are hidden within EPR line width can be often measured,[39] and two nearly identical hfs's which EPR can not distinguish can be often discriminated.[48] Thus, ENDOR is useful for purturbing the small variation of hfs constants due to the change of the electronic structure or of the molecular conformation, during the temperature variation.[55] By ELDOR also, two kinds of almost equal hf couplings of nitrogens in the DPPH[59] and the verdazyl[60] radicals could be discriminated. This results are considered to come from the difference in effective relaxation times due to the predominant electron nuclear dipolar (**END**) interactions of nitrogen atoms to those of protons. On the other hand, the proton hfs constants of the protons of the DPPH[55] and the verdazyl[57] radicals were determined by ENDOR. In addition to the features of ENDOR,

---

52 R. D. Allendoefer and D. J. Eustace, *J. Phys. Chem.*, **75**, 2765 (1971).

53 N. M. Atherton, A. J. Blackhurst, and I. P. Cook, *Trans. Faraday Soc.*, **67**, 2510 (1971); C. Steelink, J. D. Fitzpatrick, L. D. Kispert, and J. S. Hyde, *J. Amer. Chem. Soc.*, **90**, 4354 (1968); R. F. Adams and N. M. Atherton, *Mol. Phys.*, **17**, 673 (1969).

54 R. D. Allendoefer and J. H. Engelman, *Mol. Phys.*, **20**, 569 (1971).

55 N. S. Dalal, D. E. Kennedy, and C. A. McDowell, *J. Chem. Phys.*, **59**, 3403 (1973).

56 K. Mobius, H. van Willigen, and A. H. Maki, *Mol. Phys.*, **20**, 289 (1971).

57 K. Mukai, T. Yamamoto, M. Kohno, N. Azuma, and K. Ishizu, *Bull. Chem. Soc. Jpn.*, **47**, 1797 (1974).

58 R. Biehl, *Tetrahedron*, **29**, 363 (1973).

59 J. S. Hyde, R. C. Sneed, and G. H. Rist, *J. Chem. Phys.*, **51**, 1404 (1969).

60 K. Mukai, H. Shikata, N. Azuma, and K. Kuwata, *J. Mag. Res.*, **35**, 133 (1979).

mentioned above, ENDOR induced EPR[39,47] is also powerful for sorting out EPR spectra of mixed radical solution.

The ENDOR enhancement of other nuclei than protons has been possibly observed because of the effect of hyperfine enhancement[61] in spite of smaller nuclear magnetic moment of these nuclei compared with protons. The ENDOR enhancement of the nitrogen atom,[62] the carbon 13,[63] alkali- and alkaline earth metals[43,44,64] has been reported.

b) Study of the Dynamical Structure

Another important application of EPDR techniques is to study relaxations. Irradiation of mw fields can induce the coherent motion of the spin system. Thus, it induces synchronously the reversible transition of spins, that is, the reversible absorption and the reversible emission of mw energy by the spin system. However, at the same time, the spin system is subjected to various kind of magnetic interactions, randomly modulated by Brownian molecular motions. By such "spin-lattice" interactions, the spin system is really connected with the "lattice" system, the latter means the whole freedom other than the spin system. Since the lattice system is assumed to be in thermal equilibrium, mw energy is transferred irreversibly from the spin system to the lattice system. The characteristic time of this

---

61 D. H. Whiffen, *Mol. Phys.*, **10**, 595 (1966).

62 D. S. Leniart, J. C. Vedrine, and J. S. Hyde, *Chem. Phys. Lett.*, **6**, 637 (1970).

63 K. P. Dinse, K. Mobius, R. Biehl, and M. Plato, *Proc. XII Congress Ampere*, 419 (1973).

64 W. Lubitz, M. Plato, K. Mobius, and R. Biehl, *J. Amer. Chem. Soc.*, **83**, 3402 (1979).

process is called the spin lattice relaxation time (T_1). Also, such random molecular motions cause to cut off the phase coherency within the spin system, during a characteristic time, T_2, called the spin-spin relaxation time. The concepts of the T_1 and the T_2, first introduced by Bloch[65] to describe phenomeno-logically the NMR principle , are now extensively used to express relaxational characteristics, not only of magnetic resonance but also of LASER spectroscopies.[66]

The T_1 and the T_2 , or more generally, the time behavior of molecular systems can be usually studied by analyzing intensities, line widths, or even better, line shapes of the "frequency resolved" spectra. Another method of the study is to measure the "time resolved" spectra, that is, direct observation of the time dependent behavior of the system. The latter method is commonly used in recent LASER and mw spectroscopies. Also, the measurement of pulse and Fourier transformed spectra for ^{13}C has brought on a revolutionary progress to NMR spectroscopy.[67]

In the field of EPR spectroscopy, however, experimental difficulties arise from much shorter relaxation time of electron spins in contrast to moderately long relaxation time of nuclear spins. For this reason, the frequency domain measurements yet occupy the major position for studying relaxations, although the time domain measurements such as electron spin echo[68] and saturation recovery[69] have been rapidly developed in recent years. In any way, both methods are of complimentary nature, and the

---

65 F. Bloch, *Phys. Rev.*, **70**, 460 (1946).

66 K. Simoda and T. Yajima, "Quantum Electronics" Shokabou (1972).

67 T. C. Farrar and E. D. Becker, "Pulse and Fourier Transformation NMR" Academic Press Inc. (1971).

68 W. B. Mims, *Rev. Sci. Instrum.*, **36**, 1472 (1965).

unified understanding of the relaxation times determined by both methods is an important problem left in future.

ENDOR and ELDOR techniques again serve as powerful tools for studying spin relaxations in the frequency domain. Intensities and line widths of the spectra can be measured as functions of two independently irradiated mw and/or rf fields, that is, the relaxational property of radicals are examined, in a sense, stereoscopically. Their transitions are more specified than those of single resonance techniques. These features are the one which make the double resonance especially useful for the analysis of the complicated relaxation processes of actual molecular systems.

By these techniques, first of all, the mechanism of the double resonance phenomena is investigated. Several mechanisms have been proposed for ENDOR of various substances in solid state; the ΔT_{1e} mechanism,[14] the packet-shifting mechanism,[15] the distant ENDOR mechanism,[70] and the line-shift mechanism.[71]

In contrast to the relaxation mechanisms for solid state substances, that of liquid phase radicals, in which we are largely interested throughout the present study, is considered to be limited to the ΔT_{1e} mechanism.[39] In this mechanism, irradiation of rf fields brings on the change of the effective longitudinal relaxation time of electron spins, so that desaturation and resultant enhancement of the EPR intensity can be observed.

---

69 M. Huijen and J. S. Hyde, *Rev. Sci. Instrum.*, **45**, 669 (1974); "Time Domain Electron Spin Resonance" ed. L. Kevan and R. N. Schwartz John Wiley & Sons Inc. (1979).

70 J. Lambe, N. Laurance, E. C. McIrvine and R. W. Terhune, *Phys. Rev.*, **122**, 1161 (1961).

71 L. Svare and G. Seidel, *Phys. Rev.*, **134**, A 172 (1964).

The mechanism of ELDOR in liquid phase radicals is considered also to be the ΔT_{1e} mechanism due to pumping mw irradiation.[25]

1.1.3 Importance of Phenomenological Description and the Present Study

It has been established that the relaxation matrix theory developed by Freed and coworkers[72-76] describes ENDOR phenomena quite satisfactorily.[75-78] However, it is not easy to obtain an exact solution from the Freed equations even for a simple system consisting of only a few sets of equivalent protons, and even by use of a computer. Actually, most of systems with which we are concerned from the chemical point of view have several sets of equivalent protons, and we are always interesting in their characterization of proton species, their relaxational characteristics, and correlation with their molecular structure and/or electronic structure. The phenomenological theory developed in the next chapter can offer one of the easiest means for estimating double resonance effects and thus for attaining chemical purposes mentioned above.

---

72 J. H. Freed, "Electron Spin Relaxation in Liquids", ed. by L. T. Muus and P. W. Atkins, Plenum Press, New York (1972), p503.

73 J. H. Freed, *J. Chem. Phys.*, 43, 2312 (1965).

74 J. H. Freed, D. S. Leniart, and H. D. Connor, *J. Chem. Phys.*, 58, 3089 (1973).

75 J. H. Freed, *J. Phys. Chem.*, 71, 38 (1967).

76 J. H. Freed, D. S. Leniart, and J. S. Hyde, *J. Phys. Chem.*, 47, 2762 (1967).

77 D. S. Leniart, H. D. Connor, and J. H. Freed, *J. Chem. Phys.*, 63, 165 (1975).

78 N. M. Atherton and B. Day, Mol. Phys., 29, 325 (1974).

It should be noted at the present stage that phenomenological description has some value from the instructional viewpoint : Its easiness of treating allows us to describes nature straightforwardly as it shows us. Therefore one can easily understand the essence of double resonance phenomena, in other word, one can easily get a rough dessin on the phenomena, or more to say, the bird-eye-view on it. That point has been just one of the important motive forces for us to publish the present study.

The conventional phenomenological theory of magnetic resonance is based on the Bloch equations which is essentially of dynamical nature: They describe dynamics of the precessing spin system under external statical and alternating magnetic fields. Thus they have yet possibly been the basis of recent dynamical phenomena such as spin echoes. In contrast, the spin population number method, described in the next chapter, is essentially of statical nature. The both pictures can be the counterpart for expressing fully the resonance phenomena, and one would be able to bear a stereoscopic image by those understanding.

Since the relaxation processes in magnetic resonance is one manifest of the general rate processes, it may be of some value to note on an analogy of the present method with the chemical rate processes, for example, a famous system which was studied theoretically and experimentally by Bodenstein and Lind[79],

$$H_2 + Br_2 \rightarrow 2HBr\,, \qquad (1.1.2)$$

with the following reaction rate formula;

---

[79] M. Bodenstein and S. C. Lind, *Z. Phys. Chem.*, **57**,168 (1907).

$$\frac{d}{dt}[HBr] = \frac{k_a[H_2][Br_2]^{1/2}}{k_b + \frac{[HBr]}{[Br_2]}} . \qquad (1.1.3)$$

The overall reaction, (1.1.2) is known to be composed of five elementary reactions. These reactions are considered to correspond to kinds of relaxation pathways in magnetic resonance relaxation, and they are proceeded by dynamic collisions among molecular species. It should be noted that in addition to such dynamic processes, the following stationary condition is assumed:

$$\frac{d}{dt}[H] = \frac{d}{dt}[Br] = 0 \qquad (1.1.4)$$

That is, the concentration of intermediate species, H and Br, which are considered to have only a short life time is assumed to be constant in time. The present example indicates that the stationary state method is sometimes effective even for dynamic processes which proceeds with short time constant. Also, it is noted that electric circuit-like analogy may be effective in the description of rate processes in such situation.

From the above statements, one may conclude that a phenomenological theory has its own value, in spite of its somewhat lack of rigor, as long as it can explain, to a moderate extent, the experimental results for complex molecules. Therefore it is worthwhile to examine the phenomenological theory developed in the present study, by double resonance experiments, and this is just one important purpose of the present study.

The Freed theory assumes that all the hfs are completely separated. However, one often encounters cases for which the hfs is the order of the ESR line width (and for which ENDOR exhibits its full capability). In this situation, when one of the spin packets is saturated by mw irradiation, other

packets are partially saturated because of the overlapping of the packets, so that an ELDOR-like effect is brought on to reduce the ENDOR enhancement. This effect, named by us the effect of incomplete hf separation,[28] was first treated by Allendoefer and Maki,[50] who have proposed the following formula,

$$I = I_{max} \frac{T_{2e}^2 \omega_{hfs}^2}{2.5 + T_{2e}^2 \omega_{hfs}^2} \qquad (1.1.5)$$

where I_{max} is the ENDOR enhancement in the absence of the effect, ω_{hfs} is a hfs constant and T_{2e} is the spin-spin relaxation time of electron spin corresponding to the ESR linewidth. The applicability of the formula has been discussed by several either.[51,52,54,55,79,80] The beauty of the formula is its simplicity, although it has inevitable defects. A fatal difficult point is that it does not contain any relaxational term, except for T_{2e}, and therefore it is not clear under which conditions it is applicable. Indeed, as shown in Chapter 3, the ratio of the ENDOR enhancement corresponding to different proton in a molecule varies markedly with the measure-ment conditions, including especially temperature and mw power.

The phenomenological theory developed in the next chapter is a direct extension of the idea of Allendoefer and Maki. However, the present theory can describe the double resonance phenomena more comprehensively. The obtained formula can describe satisfactorily the effect of incomplete hf separation which could not been formulated by Freed, and further it is completely exempted as the simplified version of the Freed theory.

---

79 K. Ishizu, T. Yamamoto, M. Kohno, A. Nakajima, and Y. Deguchi, *Tetrahedron Lett.*, **1974**, 1537

80 K. P. Dinse, R. Biehl, and K. Mobius, *J. Chem. Phys.*, **61**, 4335 (1974).

1.2 Scope of the Thesis

Chapter 2 covers the theoretical parts of the present study. In this chapter, a phenomenological theory of EPDR is developed applying the spin population number method by Lloyde and Pake[81] and Stephan.[82]

The complete expression of the fractional ENDOR enhancement as well as the fractional ELDOR reductions are presented for a four-level system, in which all of the electron nuclear dipolar interactions, the cross relaxations, and the Heisenberg spin exchange interactions are taken into consideration. These expressions have first been developed by the present author.

The results are shown to be equivalent to those of the relaxation matrix theory developed by Freed and coworkers[72-76] except for nonlinear effects such as the coherent effect. Thus the present theory can be regarded as the simplified version of the Freed's theory.

Concerning with the ENDOR enhancement, the effect of incomplete hf separation is formulated in a general form which involves the coefficient of incomplete hyperfine separation and various kinds of transition probabilities.

Chapter 3 covers the experimental parts of the present study. In this chapter, detailed measurements of the ENDOR enhancement of galvinoxyl was performed and the results are examined with reference of the theory of EPDR developed in Chapter 2.

The results of measurement of the ELDOR reduction of galvinoxyl is described in this chapter , in comparison with the its ENDOR enhancement.

---

81 J. P. Lloyde and G. E. Pake, *Phys. Rev.*, **94**, 579 (1954).

82 M. J. Stephan, *J. Chem. Phys.*, **34**, 484 (1961).

2.1 Introduction

The time behavior of the spin system can be fully described by the density matrix theory, a kind of time dependent perturbation theory starting with the quantum-mechanical Liouville equation,

$$\frac{d\rho}{dt} = \frac{i}{\hbar}[\rho, H_0 + H(t)] , \qquad (2.1.1)$$

where ρ is the density matrix, H_0 is the time independent Hamiltonian of the zeroth order, and $H(t)$ is the time dependent Hamiltonian which includes interactions with coherent radiations as well as randomly modulated perturbations. If $\rho(t)$ can be obtained from Eq. (2.1.1), the statistical expectation value of a physical quantity, *e. g.,* magnetization can be calculated as

$$\langle M \rangle = \mathrm{Tr}\, M\rho . \qquad (2.1.2)$$

The basic idea to apply the density matrix theory for magnetic resonance was given by Bloembergen, Purcell, and Pound,[1] and was further developed by Wangness and Bloch,[2] and Bloch.[3] It was finally formulated by Redfield[4] as the Redfield relaxation matrix theory. The theory was modified by Abragam[5] and was applied by Freed and Fraenkel[6] to the analysis of

---

1 N. Bloembergen, E. M. Purcell, and R. V. Pound, *Phys. Rev.*, **73**, 679 (1948).

2 R. K. Wangness and F. Bloch, *Phys. Rev.*, **89**, 728 (1953).

3 F. Bloch, *Phys. Rev.*, **102**, 104 (1956); *ibid.*, **105**, 1206 (1957).

4 A. G. Redfield, *IBM Journal*, 19 (1957); A. G. Redfield, *Adv. Mag. Res.*, **1**, 1 (1965).

multiplet structure of EPR spectra. For ENDOR and ELDOR relaxations, thorough analysis using the method was given by Freed and coworkers in a series of papers.[7-11]

Although it is established that the Freed theory describes the double resonance relaxation quite satisfactorily, it often requires too tedious calculations so that it is difficult to apply the theory to somewhat complex molecular system in the rigorous form. Therefore it seems that there remains yet some places where the phenomenological theory is more appropriate, in cases solving practical chemical problems, in cases understanding the problem from bird eye's view, or showing problems in more simplified fashion. This is just our standpoint to perform the present investigations.

In the following, we will discuss, at first, the phenomenological treatment given by Allendoerfer and Maki.[12] Then, we will develop the spin population number method, first proposed by Lloyde and Pake,[13] and Stephan,[14] and will apply the method to double resonance relaxation in

---

5 A. Abragam, "The Principle of Nuclear Magnetism" Oxford Univ. Press (1961).

6 J. H. Freed and G. K. Fraenkel, *J. Chem. Phys.*, **39**, 326 (1963).

7 J. H. Freed, *J Chem. Phys.*, **43**, 2312 (1965).

8 J. H. Freed, *J Chem. Phys.*, **71**, 38 (1967).

9 J. H. Freed, D. S. Leniart, and J. S. Hyde, *J Chem. Phys.*, **47**, 2762 (1967).

10 J. H. Freed, D. S. Leniart, and H. D. Connor, *J Chem. Phys.*, **58**, 3089 (1973).

11 J. H. Freed, "ESR Relaxation in Liquids", ed. by L. T. Muus and P. W. Atkins (Plenum, New York) Chap. 18 (1972).

12 R. D. Allendoerfer and A. H. Maki, *J. Mag. Res.*, **3**, 396 (1970).

13 J. P. Lloyde and G. E. Pake, *Phys. Rev.*, **94**, 579 (1954).

14 M. J. Stephan, *J. Chem. Phys.*, **34**, 484 (1961).

much more general and comprehensive form than by Allendoerfer *et al.*. Thus we will calculate the theoretical ENDOR enhancement as well as the ELDOR reduction to get most general formula for a four-level system. Further we offer a simplified method to calculate them for a multi-level system.

2.2 Allendoerfer and Maki's Theory

2.2.1 Block Equations

Historically, the motion of the magnetization in external magnetic fields was first treated by Bloch[15] in NMR spectroscopy, who gave the following phenomenological equation:

$$\frac{d\boldsymbol{M}}{dt} = \gamma_e [\, \boldsymbol{M} \times (\boldsymbol{B}_0 + \boldsymbol{B}_1) \,] - \frac{(M_x \mathbf{i} + M_y \mathbf{j})}{T_{2e}} - \frac{(M_z - M_0)\,\mathbf{k}}{T_{1e}} \qquad (2.2.1)$$

where γ_e is the gyromagnetic ratio of electron spins, $\boldsymbol{M}$ is the magnetization, $\boldsymbol{B}_0$ is the static magnetic flux, $\boldsymbol{B}_1$ is the alternating magnetic flux, and $\mathbf{i}$, $\mathbf{j}$, $\mathbf{k}$ are unit vectors in the laboratory coordinate system. The fundamental assumption in this equation is that the magnetization precesses under the tork generated by the external magnetic flux densities, $\boldsymbol{B}_0$ and $\boldsymbol{B}_1$, that the z component of the magnetization relaxes exponentially to its thermal equilibrium value,

$$M_0 = \chi_0 B_0 ,^{*} \qquad (2.2.2)$$

---

15 F. Bloch, *Phys. Rev.*, 70, 460 (1946).

with a characteristic time T_{1e} (longitudinal relaxation time), and that the x- and y components of the magnetization relaxes to zero with a characteristic time, T_{2e} (transverse relaxation time). If we choose coordinate system, rotating with the mw frequency, w_e, the steady state solution of Eq. (2.2.1) can be obtained as

$$u = M_0 \frac{\gamma_e B_1 T_{2e}^2 (\omega_{e0} - \omega_e)}{1 + T_{2e}^2 (\omega_{e0} - \omega_e)^2 + \gamma_e^2 B_1^2 T_{1e} T_{2e}}, \tag{2.2.3}$$

$$v = M_0 \frac{\gamma_e B_1 T_{2e}}{1 + T_{2e}^2 (\omega_{e0} - \omega_e)^2 + \gamma_e^2 B_1^2 T_{1e} T_{2e}}, \tag{2.2.4}$$

$$M_z = M_0 \frac{1 + T_{2e}^2 (\omega_{e0} - \omega_e)^2}{1 + T_{2e}^2 (\omega_{e0} - \omega_e)^2 + \gamma_e^2 B_1^2 T_{1e} T_{2e}}, \tag{2.2.5}$$

where

$$\boldsymbol{B}_1 = B_1 \cos \omega_e t\, \mathbf{i} - B_1 \sin \omega_e t\, \mathbf{j}, \tag{2.2.6}$$

$$\boldsymbol{M} = (u \cos \omega_e t + v \sin \omega_e t)\, \mathbf{i} + (u \sin \omega_e t - v \cos \omega_e t)\, \mathbf{j} + M_z \mathbf{k} \tag{2.2.7}$$

and ω_{e0} is the Larmor frequency given by

$$\omega_{e0} = \gamma_e B_0 . \tag{2.2.8}$$

2.2.2 Allendoerfer and Maki's Theory

Allendoerfer and Maki's treatment[12] starts with the derivative form of the

---

* We represent by $\boldsymbol{M}$'s the magnetization divided by permeability μ, so that its unit is given by T (tesla), and that χ_0 has unit, 1. Also γ_e should have a unit, rad s^{-1} T^{-1} in the same context.

EPR absorption shown in Eq. (2.2.4).

$$\frac{\partial \nu}{\partial \omega_e} = M_0 \frac{2\gamma_e B_1 T_{2e}^3 (\omega_{e0} - \omega_e)}{\{1 + T_{2e}^2(\omega_{e0} - \omega_e)^2 + \gamma_e^2 B_1^2 T_{1e} T_{2e}\}^2} \qquad (2.2.9)$$

The peak intensity of the derivative absorption is then obtained from the value of ω_e which makes $\frac{\partial^2 \nu}{\partial \omega_e^2} = 0$, as

$$I_{EPR} = \left[\frac{\partial \nu}{\partial \omega_e}\right]_{max}$$

$$= \frac{3\sqrt{3}}{8} M_0 \frac{\gamma_e B_1 T_{2e}^2}{(1 + \gamma_e^2 B_1^2 T_{1e} T_{2e})^{3/2}} \qquad (2.2.10)$$

The basic idea is that, as Seidel had already indicated,[16] rf irradiation brings on a shortening of the effective T_{1e}, which results in desaturation of the previously saturated EPR line so as to increase of the EPR intensity. Thus, the ENDOR enhancement is calculated as a function of mw power from

$$I_{ENDOR} = \frac{\partial}{\partial T_{1e}}\left[\frac{\partial \nu}{\partial \omega_e}\right]_{max} \Delta T_{1e}$$

$$= \frac{9\sqrt{3}}{16} M_0 \frac{\gamma_e^3 B_1^3 T_{2e}^3 \Delta T_{1e}}{(1 + \gamma_e^2 B_1^2 T_{1e} T_{2e})^{5/2}} \cdot \qquad (2.2.11)$$

Also, Allendoerfer and Maki formulated the dependence of the ENDOR enhancement on rf power, assuming a relaxation time caused from the rf-induced transitions as

$$T_i^{-1} = \frac{\gamma_n^2 B_2^2 T_{1n}^2}{1 + \gamma_n^2 B_2^2 T_{1n}^2}, \qquad (2.2.12)$$

---

16 H. Seidel, *Z. Physik*, 165, 218 (1961).

although validity of this equation is not somewhat clear. In the above, γ_n and T_{1n} are the gyromagnetic ratio and the longitudinal relaxation time of nuclear spins, respectively.

The most attractive result from the Allendoerfer and Maki's treatment is on the relation lying between the magnitudes of the hf coupling and the ENDOR enhancement. It is experimentally known that the relative intensity of the ENDOR enhancement for different proton in a molecule decreases as its hfs decreases, if other conditions such as the nuclear spin relaxation mechanism are the same. Such tendency is most prominent for protons whose hfs's are as small as the EPR line width, so only an weak ENDOR enhancement can be observed for these protons.

The effect, which was named by us "the effect of incomplete hyperfine separation",[17] is understood as follows: Consider a proton whose hfs is enough small that the spin packets corresponding to the 1, 2- and 3, 4- levels are overlapping (See Fig. 2-1 (c)). Then the spin packet for 3, 4- levels will be partially saturated, as that for 1, 2- levels is saturated by the observing mw irradiation. The population difference between spins on the 1- and the 3- levels is naturally decreased, so that the ENDOR effect for these levels is decreased.

Allendoerfer and Maki assumed that the ENDOR enhance-ment in the presence of this effect is proportional to the difference, ΔM_z, between the two M_z's, corresponding to the 1, 2- levels and the 3, 4- levels, respectively, thus,

$$\Delta M_z = M_z(3,4) - M_z(1,2) \quad . \tag{2.2.13}$$

From Eq. (2.2.11), it is shown that the ENDOR enhancement is optimized at

---

[17] H. Shikata, Bull. Chem. Soc., 50, 3084 (1977).

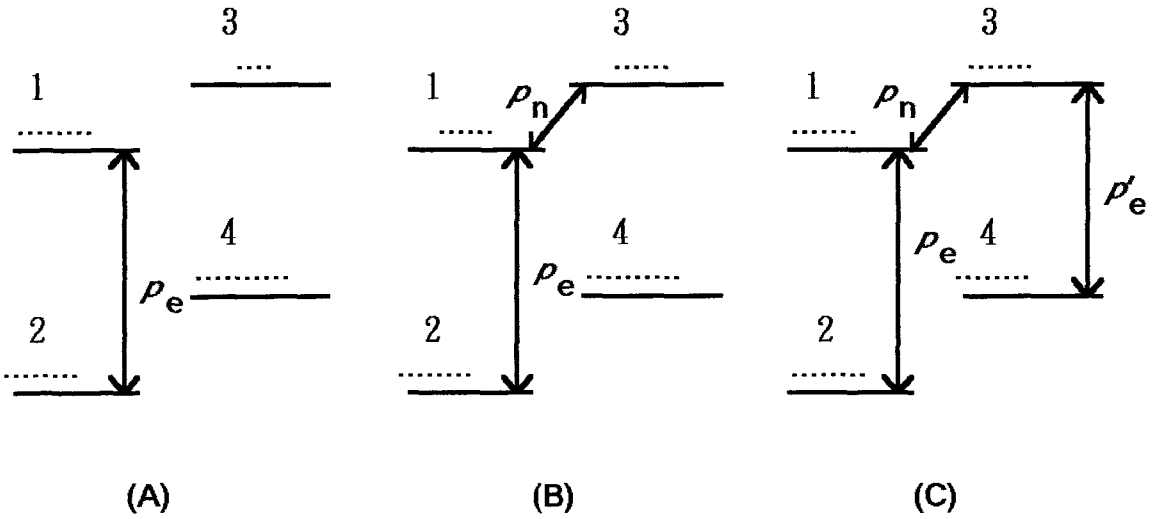

Fig. 2-1 Schematic diagram of the effect of incomplete hyperfine separation for a four-level system. Dots represent spin population.

(A) EPR :1-level is partially saturated.

(B) ENDOR, Large hfs case : 1- and 3- levels are equalized by ρ_n, so that 1-level is desaturated.

(C) ENDOR, Small hfs case (Effect of incomplete hyperfine separation): 3- and, 4 levels are partially equalized by ρ'_e, so that difference between 1- and 2- levels is decreased than in (B).

the mw power which satisfies

$$\gamma_e^2 B_1^2 T_{1e} T_{2e} = \frac{3}{2} . \qquad (2.2.14)$$

Then employing this value of mw power at the resonance point of 1- and 2-levels, we obtain from Eq. (2.2.5),

$$\Delta M_z = M_0 \{ \frac{1 + T_{2e}^2 \omega_{hfs}^2}{1 + T_{2e}^2 \omega_{hfs}^2 + \gamma_e^2 B_1^2 T_{1e} T_{2e}} - \frac{1}{1 + \gamma_e^2 B_1^2 T_{1e} T_{2e}} \}$$

$$= \frac{3}{5} M_0 \frac{T_{2e}^2 \omega_{hfs}^2}{2.5 + T_{2e}^2 \omega_{hfs}^2} \qquad (2.2.15)$$

ω_{hfs}^2 is the hfs constant in angular frequency. Thus we obtain the ENDOR enhancement in the presence of the effect of incomplete hf separation as

$$F = F_{max} \frac{T_{2e}^2 \omega_{hfs}^2}{2.5 + T_{2e}^2 \omega_{hfs}^2}, \qquad (2.2.16)$$

where F_{max} is the ENDOR enhancement in the absence of this effect. The transverse relaxation time, T_{2e}, in this equation is usually estimated from the EPR line width by

$$T_{2e} = \frac{2}{\sqrt{3} \gamma_e \Delta B_{pp}}, \qquad (2.2.17)$$

where ΔB_{pp} is the peak-to-peak width of the derivative EPR line. However the value of T_{2e} is usually rather tentatively chosen in the range, 0.1s - 1s, because in many cases EPR spectra are inhomogeneously broadened.

2.3 Theory of Electron Paramagnetic Double Resonance Based on Spin Population Number Method.*

2.3.1 Transition Probabilities

When the spin system is exposed under the external and/or internal time-dependent magnetic fields, it will interact with these fields, and then , if the frequency component of the Fourier spectrum of interaction satisfies the Bohr's frequency condition,

$$E_{s2} - E_{s1} = \hbar\omega \ , \tag{2.3.1}$$

they will rise on many types of transitions. From the view point of their reversibility, transitions may be classified into two . One is the photon-type transitions which is induced by the coherent electromagnetic fields. They have intrinsic reversibility, as fundamentally assured by quantum mechanics.

$$P_{\uparrow} = P_{\downarrow} \tag{2.3.2}$$

The other is the phonon-type transitions which is induced by so-to-speak the incoherent electromagnetic fields: The magnetic perturbations are randomly modulated by the lattice motions, so that if their spectra have appropriate frequency components for spin transition as in Eq. (2.3.1) and at the same time, have non-vanishing matrix element between the two states,

---

* The parts of the present section have already been published in H. Shikata, *Bull. Chem. Soc. Jpn.*, **50**, 3084-3089 (1977), as the title, "A Phenomenological Description of Electron Paramagnetic Double Resonance Relaxation of Organic Free Radicals in Solution. I. Theory of ENDOR Based on the Spin-Population Number Method".

transitions should be induced by these fields. Such a process may be treated, at least indirectly, by thermodynamics or statistical thermodynamics, considering that the spin system is connected to the lattice system having infinite freedom or infinite heat capacity. Therefore such coupling between the spin system and the lattice system will lead to irreversibility of the lattice-induced transition probabilities which is ultimately expressed by the Boltzmann relation.

$$W_{\uparrow} = W_{\downarrow} \exp(-\frac{E_{s2} - E_{s1}}{kT}) \qquad (2.3.3)$$

The quite contrast character as for reversibility mentioned above brings on different role to the two type of transition probabilities: The role of alternating field-induced transition probabilities, P's, is thought to be that of making a partial short-circuit over the spin relaxation pathways, which necessarily decreases the difference in the spin population numbers of the two spin levels between which spins make transition. On the other hand, the role of the lattice-induced transition probabilities, W's, is to be that of keeping the spin system Boltzmann distribution. These transition probabilities are formulated in the following.

a) Lattice-Induced Transition Probabilities

When the spin system is excited by the external radiations, it will attain to a temperature higher than the lattice temperature. Then the energy of the spin system will transfer to the lattice system, if the both systems are coupled by perturbations called the spin-lattice interaction. The frequency of spin transition through this process is called the lattice-induced transition probability; Such processes are characterized both by the magnitude of

spin-lattice interactions and the time constants of molecular motions.

If we treat a total system which includes both spin freedom and lattice freedom, we can describe, in princple, the motion of the system by use of master equations of Redfield. [4]

$$\frac{d}{dt}\sigma^*_{bb'} = \sum_{bb'} R'_{aa',bb'}\sigma^*_{bb'} \quad , \tag{2.3.4}$$

However, since actual system has too much freedom to apply directly the above equation, we must introduce a method in which the lattice Hamiltonian is not explicitly considered. Such a method have necessarily, in a sense, of phenomenological character. An achievement of thermal equilibrium may be described by either of two kind of method.

In one method, it is assumed that randomly modulated perturbations turn out the same magnitude of flip and flop transition probabilities of spins, and further for the sake of attaining thermal equilibrium, the density of the spin system is postulated to vary with time in proportion to the discrepancy from the density at thermal equilibrium.

$$\frac{d}{dt}\sigma^*_{bb'} = \sum_{bb'} R'_{aa',bb'}(\sigma^*(t) - \sigma^*_0)_{bb'} \quad , \tag{2.3.5}$$

where

$$\sigma^*_0 = \frac{\exp -\frac{\hbar H_0}{kT}}{\mathrm{Tr}\{\exp -\frac{\hbar H_0}{kT}\}} \tag{2.3.6}$$

is the density operator of the spin system at thermal equilibrium with H_0 as the non-perturbation Hamiltonian of this system. $\sigma^*(t)$ is the density

operator at a time, t, R's are the relaxation matrices, * means the interaction representation, and Σ' means the summation satisfying the energy relation,

$$b - b' = a - a' . \tag{2.3.7}$$

In another method which we employ in the present theory, a rate equation for a steady state are assumed corresponding to diagonal elements of Eq. (2.3.4). Furthermore, but it is assumed that the flip and flop transition probabilities induced by the lattice motion are connected by the Boltzmann relation. The latter assumption is justified as follows:[5]

If we denote the lattice state by $|f\rangle$ with its energy by E_f, the probability that the lattice is found in the state, $|f\rangle$, is proportional to the Boltzmann factor, $\exp\frac{-E_f}{kT}$. The transitions of spin state comprise of the summation of the combined spin-lattice transitions, whose probabilities are denoted by $W_{f,s\to f',s'}$, at which energy should be conserved;

$$E_f + E_s = E_{f'} + E_{s'} \tag{2.3.8}$$

as well as

$$W_{f,s\to f',s'} = W_{f',s'\to f,s} \tag{2.3.9}$$

is satisfied from the general principle of the quantum mechanics. Then,

$$\frac{W_{s\to s'}}{W_{s'\to s}} = \frac{\sum_{f,f'}\exp(-E_f/kT)\,W_{f,s\to f',s'}}{\sum_{f,f'}\exp(-E_{f'}/kT)\,W_{f',s'\to f,s}} = \exp\frac{-(E_{s'}-E_s)}{kT} \tag{2.3.10}$$

In the following, we denote the transition probabilities induced by the lattice as W's. These are classified largely into three (See Fig. 2.1)

a) Electron spin transitions

W_e ($\Delta M_S = \pm 1$, $\Delta M_J = 0$)

b) Combined electron spin - nuclear spin transitions

W_{x1} ($\Delta M_S = \pm 1$, $\Delta M_J = \pm 1$)

W_{x2} ($\Delta M_S = \pm 1$, $\Delta M_J = \mp 1$)

c) Nuclear spin transition

W_n ($\Delta M_S = 0$, $\Delta M_J = \pm 1$)

From the above arguments, we assume for the first three kinds of transition probabilities which satisfy $\Delta M_S = \pm 1$, under high temperature approximation,

$$\frac{W_{\uparrow}^{(e)}}{W_{\downarrow}^{(e)}} = \exp \frac{-\gamma_e \hbar B_0}{kT} \fallingdotseq 1 - \varepsilon_e , \tag{2.3.11}$$

where

$$\varepsilon_e = \frac{\gamma_e \hbar B_0}{kT} \tag{2.3.12}$$

Also, we assume for the nuclear spin transition probabilities,

$$\frac{W_{\uparrow}^{(n)}}{W_{\downarrow}^{(n)}} = \exp \frac{-\gamma_n \hbar B_0}{kT} \fallingdotseq 1 - \varepsilon_n , \tag{2.3.13}$$

where

$$\varepsilon_n = \frac{\gamma_n \hbar B_0}{kT} \tag{2.3.14}$$

In case that we are observing EPR, we may set

$$W_{n\uparrow} = W_{n\downarrow} \tag{2.3.15}$$

because the nuclear Zeeman interaction and the hf interactions are so small as to bear a net population difference of the electron spin levels.

b) Microwave- and Rf-Induced Transition Probabilities

The transverse relaxation time, T_{2e} found in Eq. (2.2.1) is known to have two types of terms:

$$\frac{1}{T_{2e}} = \frac{1}{T'_{2e}} + \frac{1}{2T_{1e}} \,. \tag{2.3.16}$$

The first term is called the secular broadening, because it is related to the z component of the fluctuation fields. The zero frequency component of its power spectrum brings on a sudden change of the Larmor frequency

$$\omega_{e0} = \gamma_e B_0 \,, \tag{2.3.17}$$

that is, it cuts off the coherent motion of the magnetization in a time, T_{2e}. Also, the second term in Eq. (2.3.16) is called the nonsecular broadening, because it is related to the x and y component of fluctuating fields. Their spectral density oscillating at frequency, ω_{e0}, brings on transition of the spin state, or the limited life-time of the spin state, or further, the uncertainty of the spin energy. The coherent motion of the magnetization is again cut off in a time, T_{1e}, by this "life-time broadening mechanism". Now we illustrate that such limited phase coherency of the spin states leads to a Lorentzian shape

function for the transition probabilities induced by the coherent radiations.[18] Let us consider a simple two-level system whose zeroth order wave functions and energies are represented by (Ψ_1^0, $\hbar\omega_1$) and (Ψ_2^0, $\hbar\omega_2$) and

write the Hamiltonian of the system as

$$H = H_0 + H' \tag{2.3.18}$$

where H_0 is the zeroth Hamiltonian and

$$H' = V e^{-i\omega t} \tag{2.3.19}$$

is a time-dependent perturbation resulting from the coherent radiation whose diagonal terms are assumed to be zero. We seek a solution of the time-dependent Schrodinger equation

$$i\hbar \frac{\partial \Psi}{\partial t} = (H_0 + H') \Psi , \tag{2.3.20}$$

in the form of a sum,

$$\Psi(t) = C_1(t) \psi_1^0 e^{-i\omega_1 t} + C_2(t) \psi_2^0 e^{-i\omega_2 t} . \tag{2.3.21}$$

Substituting this equation to Eq. (2.3.20), multiplying both sides by $\psi_2^{0*} e^{i\omega 2 t}$, and integrating over coordinate space, we have

$$i\hbar \frac{d}{dt} C_2(t) = \langle 2 | H' | 1 \rangle \; C_1(t) e^{i\omega_1 t}, \tag{2.3.22}$$

where $C_1(0) = 1$ with $C_2(0) = 0$ is assumed and $\omega_0 = \omega_2 - \omega_1$.

---

18 K. Shimoda and T. Yajima, "Quantum Electronics" Shokabo (1972).

Now we assume that fluctuating perturbations diminish coherency of the initial state exponentially with a time T_2;

$$C_1(t) = C(0) \exp\left(-\frac{t}{T_2}\right) \tag{2.3.23}$$

Then

$$C_2(t) = \frac{\langle 2 \mid V \mid 1 \rangle \{1 + \exp i\left(\omega - \omega_0 + \frac{i}{T_2}\right) t\}}{\hbar\left(\omega - \omega_0 + \frac{i}{T_2}\right)} \tag{2.3.24}$$

Setting the frequency width by $2/T_2$, we obtain the transition probability from the state 1 to 2 after enough long time that $t \gg T_2$ as

$$P_{12} = \int C_2(\infty) \mid^2 d\rho_2 \fallingdotseq \frac{2}{T_2} \frac{\mid \langle 2 \mid V \mid 1 \rangle / \hbar \mid^2}{(\omega - \omega_0)^2 + 1/{T_2}^2}, \tag{2.3.25}$$

where ρ_2 is the density of energy levels in unit frequency.

The result shows that the transition probability induced by coherent radiation is a Lorentzian function with $1/T_2$ as the half width at half maximum.

The Lorentzian line shape is commonly seen in the resonance system in which energy is dissipated as the form of the dumped oscillation, such as in LCR tuning circuit in electronics. The natural line widths in optical spectroscopy is also understood similarly.[19]

From the above discussion, we assume the following expressions for the transition probabilities induced by the mw and rf fields: When the mw magnetic field, $2B_1 \cos \omega_e t$ is applied,

---

19 V. W. Weisskopf and E. Wigner, *Z. Physik*, **63**, 54 (1930).

$$P_e = \frac{1}{2}\gamma_e^2 B_1^2 T_{2e} \mid \langle \frac{1}{2} \mid S_+ \mid -\frac{1}{2} \rangle \mid^2 \frac{1}{1 + T_{2e}^2(\omega_{e0} - \omega_e)^2}, \quad (2.3.26)$$

and when the rf magnetic field $2B_2 \cos \omega_n t$ is applied,

$$P_n = \frac{1}{2}\gamma_n^2 B_2^2 T_{2n} \mid \langle M_J \mid J_+ \mid M_{J-1} \rangle \mid^2 \frac{1}{1 + T_{2n}^2(\omega_{n0} - \omega_n)^2}, \quad (2.3.27)$$

where γ_e and γ_n are the gyromagnetic ratio of the electron- and nuclear spins, T_{2e} and T_{2n} are the transverse relaxation times, ω_{e0} and ω_{n0} are the resonant angular frequencies, and S_+ and J_+ are the lifting operators of, respectively, the electron- and nuclear spins.

It is convenient for later discussion to express transition probabilities by the ratio to We using small letter notation, thus

$$w = W/W_e,\ b = W_n/W_e,\ b_{x1} = W_{x1}/W_e,$$

$$b_{x2} = W_{x2}/W_e,\ p_e = P_e/W_e,\ p_n = P_n/W_e\ . \quad (2.3.28)$$

p_e is a very convenient quantity, representing mw power, that is, at the EPR resonance point,

$$p_e = \frac{\gamma_e^2 B_1^2 T_{2e}}{2W_e} = \gamma_e^2 B_1^2 T_{1e} T_{2e} \quad (2.3.29)$$

At the EPR maximum, p_e = 1/2 and at the ENDOR maximum, p_e = 3/2 (See Eqs. (2.3.78) and (2.3.79)).

2.3.2 Equations Governing Spin Population Numbers

We can interpret the diagonal elements of the Redfield equation, Eq. (2.3.4), to be the master equation governing the spin population. By analogy to this equation, we assume the following first order rate equation for the transition velocities of the spin population numbers keeping on a stationary state, thus

$$\frac{\mathrm{d}\boldsymbol{N}}{\mathrm{d}t} = \boldsymbol{C}\boldsymbol{N} = 0 \ , \tag{2.3.30}$$

where $\boldsymbol{N} = \{N_i\}$ is the spin population number of each spin level, in which case the total spin population number should be conserved:

$$\sum_i N_i = N . \tag{2.2.31}$$

$\boldsymbol{C}$ is a conduction matrix composed of various kinds of both lattice-induced and radiation induced transition probabilities.

Eq. (2.3.30) implicitly requires the condition that the external radiations are not so strong as to allow the neglect of multi-quantum transition processes such as the coherent effects.[8] Also this condition is necessary for Eqs. (2.3.26) and (2.3.27), because if it is not satisfied, the saturated Lorentzian form should be adopted in place of the Lorentzian in these equations.

2.3.3 EPR Absorption and Double Resonance Effects

When an alternating field, $2B_1\cos w_e t$ is applied to a paramagnetic system, we have the following magnetization as the in-phase and out-of-phase response of the system:

$$M_x = \mathrm{Re}\,(c'B_1 e^{i\omega_e t}), \tag{2.3.32}$$

where

$$\chi = \chi' - i\chi'' \tag{2.3.33}$$

is the complex magnetic susceptibility and Re means the real part. As the result of the interaction between M_x and B_1 field, energy is absorbed from the field[20] at an average rate,

$$A = \frac{\omega_e}{2\pi}\int_0^{2\pi/\omega_e} 2B_1\cos\omega_e t\,\frac{dM_x}{dt}\,dt$$

$$= 2\omega_e\chi''B_1^2 . \tag{2.3.34}$$

On the other hand the photon energy absorbed by the system is given by,

$$A = nP_e\hbar\omega_e , \tag{2.3.35}$$

where n is the difference in the spin population numbers between the two levels at which EPR is observed. Since n can be readily obtained from Eqs. (2.3.27) and (2.3.28), from the above two equations, we can estimate the EPR absorption and the double resonance effects on it, which are defined as follows:

---

20 D. J. E. Ingram, "Free Radicals as Studied by Electron Spin Resonance", Butterworths (1958).

(i) Integral intensity of EPR absorption

$$I = \chi'' B_1 \tag{2.3.36}$$

(ii) Peak intensity of the first derivative of EPR absorption

$$I_{EPR} = \left[\frac{\partial I}{\partial \omega_e}\right]_{max} \tag{2.3.37}$$

(iii) ENDOR enhancement

$$I_{ENDOR} = I_{EPR}(ON) - I_{EPR}(OFF) \tag{2.3.38}$$

(IV) Fractional ENDOR enhancement

$$E = \frac{I_{ENDOR}}{I_{EPR}(OFF)} \tag{2.3.39}$$

(v) ELDOR reduction

$$I_{ELDOR} = I_{EPR}(OFF) - I_{EPR}(ON) \tag{2.3.40}$$

(vi) Fractional ELDOR reduction

$$R = \frac{I_{ELDOR}}{I_{EPR}(OFF)} \tag{2.3.41}$$

where in Eqs. (2.3.38) and (2.3.39), ON denotes rf irradiation and OFF the absence of rf power, whereas in Eqs. (2.3.40) and (2.3.41) ON denotes pumping mw power irradiated and OFF its absence.

2.3.4 Two-Level System

We start our discussion in this section by treating a most simple two-level system shown in Fig. 2.2 in order to illustrate the present method. We have

$$\frac{d N_1}{d t} = - (P_e + W_{e\downarrow}) N_1 + (P_e + W_{e\uparrow}) N_2 = 0 \tag{2.3.42}$$

or

$$\begin{bmatrix} -(1 + \rho_e) & (1 - e) + \rho_e \\ (1 + \rho_e) & -\{(1 - e) + \rho_e\} \end{bmatrix} \begin{bmatrix} N_1 \\ N_2 \end{bmatrix} = 0 \tag{2.3.43}$$

Denoting

$$n = N_2 - N_1 \tag{2.3.44}$$

and

$$N = N_1 + N_2 \tag{2.3.45}$$

or

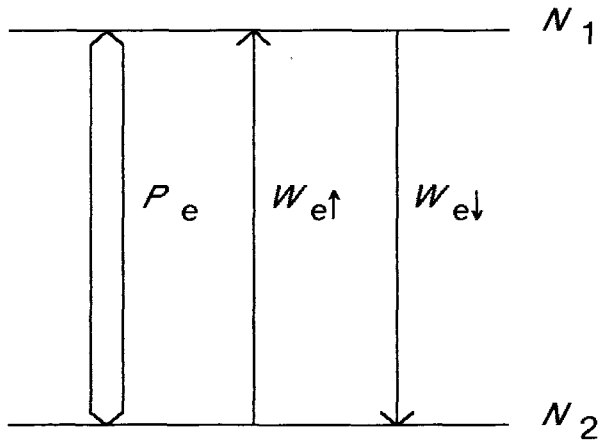

Fig. 2.2 Two-level System

$$\begin{bmatrix} N_1 \\ N_2 \end{bmatrix} = \frac{1}{2}\begin{bmatrix} -1 & 1 \\ 1 & 1 \end{bmatrix}\begin{bmatrix} n \\ N \end{bmatrix}, \tag{2.3.46}$$

and substituting to the above equation, we obtain

$$n = \frac{1}{1 + \rho_e} n_0 . \tag{2.3.47}$$

where

$$n_0 = \frac{\varepsilon_e N}{2} = \frac{N\gamma_e \hbar B_0}{2kT} \tag{2.3.48}$$

is the difference in spin population numbers in thermal equilibrium. The energy absorbed in unit time from the mw radiation is given from Eq.(2.3.35) by

$$A = n_0 \hbar\omega_e \frac{\rho_e}{(1 + \rho_e)} W_e \tag{2.3.49}$$

Using Eqs, (2.3.34) and (2.3.36) , we obtain a saturated Lorentzian form for the integral intensity of EPR absorption as

$$I = \frac{1}{2}\chi_0 B_0 \frac{\gamma_e B_1 T_{2e}}{1 + T_{2e}^2(\omega_{e0} - \omega_e)^2 + \gamma_e^2 B_1^2 T_{1e} T_{2e}} , \tag{2.3.50}$$

where χ_0 is the static magnetic susceptibility related to the static magnetization, M_0 and n_0 by

$$M_0 = \chi_0 B_0 = \frac{\gamma_e \hbar n_0}{2} = \frac{N\gamma_e^2 \hbar^2}{4kT} . \tag{2.3.51}$$

$$T_{1e} = \frac{1}{2W_e} . \tag{2.3.52}$$

is the longitudinal relaxation time of an electron spin.

2.3.5 Four-Level System

a) Resonance Frequency

We proceed to a four-level system as shown in Fig. 2.3. The system is composed of an electron, having its electron spin with $S = 1/2$ and $M_S = \{1/2, -1/2\}$, and a proton, having its (total) nuclear spin with $J = 1/2$ and $M_J = \{1/2, -1/2\}$. In addition, the both ared coupled with a hyperfine interaction, ω_{hfs}. From the spin hamiltonian of this system,

$$H_0 / \hbar = \gamma_e SB_0 + \gamma_n JB_0 + \omega_{hfs} JS. \qquad (2.3.53)$$

Then two peaks are expected by EPR and ELDOR at frequency,

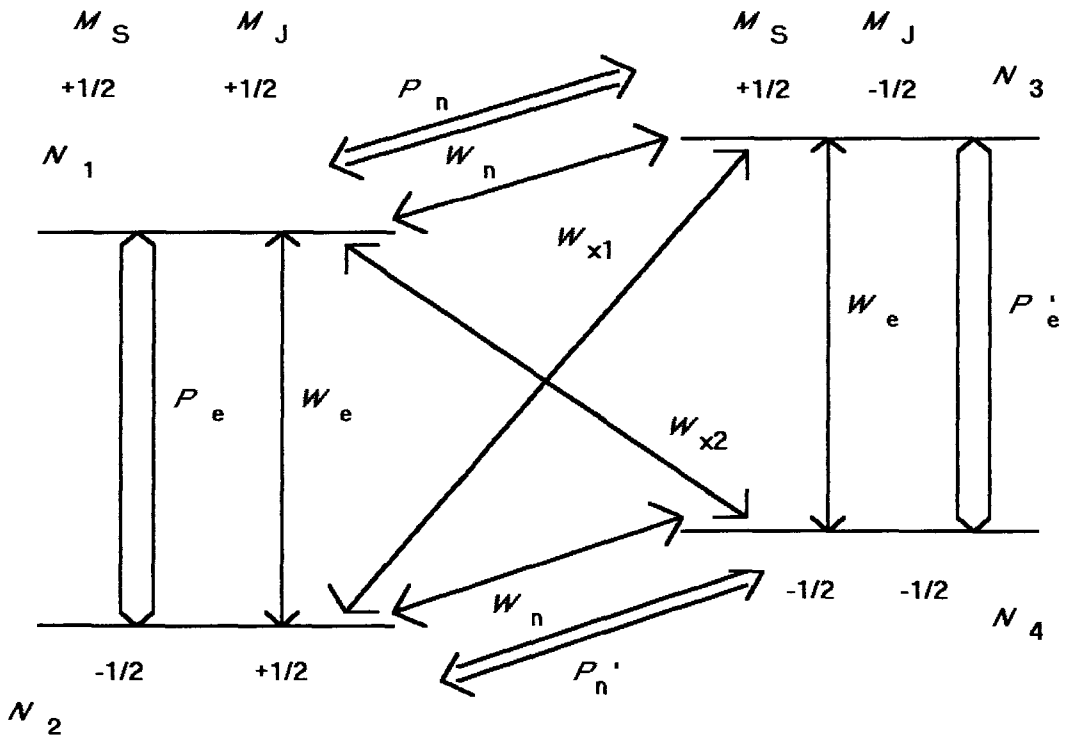

Fig. 2.3 Schematic diagram of the energy levels and the transition probabilities for a four-spin-level system.

$$\omega_{e0} = \gamma_e B_0 \pm \frac{1}{2}\omega_{hfs} \tag{2.3.54}$$

Also, two NMR transitions may be observed at frequency

$$\omega_{n0} = |\gamma_n B_0 \pm \frac{1}{2}\omega_{hfs}|, \tag{2.3.55}$$

by ENDOR, single NMR, and NEDOR.

b) Spin Population Number

In the above figure, the spin population number of each level is governed by four kinds of the lattice induced transition probabilities, W_e, W_{x1}, W_{x2}, and W_n, as well as by four kinds of alternating field-induced transition probabilities, P_e, P'_e, P_n, P'_n, which are singly or plurally irradiated simultaneously.

If 1, 3- or 2, 4- transitions are excited by rf irradiation with ρ_n or ρ'_n, during monitoring the 1, 2-transition with ρ_e, we observe two peaks of ENDOR enhancement. Also simultaneous irradiation of both means TRIPLE enhancement. If the proton hfs is sufficiently small that the effect of incomplete hyperfine separation occurs, ENDOR enhancement will be somewhat diminished by the presence of ρ'_e, On the other hand, if we pump 3,4- levels by mw excitation we can expect ELDOR reduction. Also, if we observe transition between 1,3- levels, during irradiation of mw between 1,2- levels or 3,4- levels, then tjis will be a NEDOR experiment.

Now the spin occupation numbers on each spin level are given by

$$N = \begin{bmatrix} N_1 \\ N_2 \\ N_3 \\ N_4 \end{bmatrix}, \tag{2.3.56}$$

which satisfies the conservation relation,

$$\sum_{i=1}^{4} N_i = N. \tag{2.3.57}$$

Defining the difference in the spin population numbers by

$$n = n_{12} = N_2 - N_1, \tag{2.3.58}$$

$$n_{34} = N_4 - N_3, \tag{2.3.59}$$

$$n_{13} = N_3 - N_1. \tag{2.3.60}$$

the vector N can be related to the difference vector including N, as follows:

$$\begin{bmatrix} N_1 \\ N_2 \\ N_3 \\ N_4 \end{bmatrix} = \frac{1}{4} \begin{bmatrix} -1 & -1 & -2 & 1 \\ 3 & -1 & -2 & 1 \\ -1 & -1 & 2 & 1 \\ -1 & 3 & 2 & 1 \end{bmatrix} \begin{bmatrix} n \\ n_{34} \\ n_{13} \\ N \end{bmatrix}. \tag{2.3.61}$$

c) Heisenberg Spin Exchange Effect

It will be appropriate at the present stage to introduce the transition probability due to the Heisenberg spin exchange effect, in order to obtain the most general expression for the difference in the spin population numbers of a four-level system. We shall analyses the problem according to the Freed's

suggestion on the Heisenberg exchange effect[4] with the strong collision approximation.

There exists six types, a - f, of collisions between the spins on the two of four levels as listed in Table 2.1. Though the electron spin state loses its memory by all these collisions with 1/2 probability, a - d type collisions bring on no different spin state than that before collision. However e and f type collisions can change the spin state *i.e.,* can result in the effective spin transitions . That is, a collision between 1, 4-level spins eliminates both spins and generates 2, 3-level spins and *vice versa* . Thus the Heisenberg exchange effect can be considered to bring on the equality of spin population of 1, 2-levels or 2, 4-levels by increase of effective cross transitions. Consequently, the transition velocity of the spin population numbers of each spin level due to the Heisenberg spin exchange is represented as follows:

$$\left[\frac{dN_1}{dt}\right]_{HE} = -\left[\frac{dN_2}{dt}\right]_{HE} = -\left[\frac{dN_3}{dt}\right]_{HE} = \left[\frac{dN_4}{dt}\right]_{HE}$$

$$= W_{HE}(N_2N_3 - N_1N_4) = \frac{1}{2}w_{HE}(n - n_{34}), \qquad (2.3.62)$$

In the above equation, Eq. (2.3.61) is substituted and estimated to the first order of the population difference. We represent the Heisenberg exchange frequency,

$$\omega_{HE} = \frac{NW_{HE}}{2} \qquad (2.3.63)$$

and

Table 2.1 Collision among spins on four spin-levels

	Colliding pair		Spin state after collision	
	M_S M_J	M_S M_J	M_S M_J	M_S M_J
a	(+1/2, +1/2)	(-1/2, +1/2)	(-1/2, +1/2) & (+1/2, +1/2)	
b	(+1/2, -1/2)	(-1/2, -1/2)	(-1/2, -1/2) & (+1/2, -1/2)	
c	(+1/2, +1/2)	(+1/2, -1/2)	(+1/2, +1/2) & (+1/2, -1/2)	
d	(-1/2, +1/2)	(-1/2, -1/2)	(-1/2, +1/2) & (-1/2, -1/2)	
e	~~(-1/2, +1/2)~~	~~(+1/2, -1/2)~~	~~(+1/2, +1/2) & (-1/2, -1/2)~~	
f	~~(+1/2, +1/2)~~	~~(-1/2, -1/2)~~	~~(-1/2, +1/2) & (+1/2, -1/2)~~	

$$b' = \frac{\omega_{HE}}{W_e} \tag{2.2.64}$$

Then we obtain

$$\frac{dN}{dt} = \left[\frac{dN}{dt}\right]_0 + \left[\frac{dN}{dt}\right]_{HE} \tag{2.3.65}$$

The above method can be easily applied to the system in which chemical exchange effect plays important role.

d) Conduction Matrix

From the above consideration, we obtain the most general conduction matrix of a four-level system for the rate equation,

$$CN = 0\,, \tag{2.3.66}$$

$$C = C_0 + C_{HE} \tag{2.3.67}$$

Using notations in (2.3.28),

$$C_0 =$$

$$\begin{bmatrix} -\{1+(1-\varepsilon_n)b + b_{x2} + p_e + p_n\} & 1-\varepsilon_e + p_e & b + p_n & (1-\varepsilon_e)b_{x2} \\ 1+p_e & -\{(1-\varepsilon_e)(1+b_{x1}) + (1-\varepsilon_n)b + p_e + p'_n\} & b_{x1} & b+p'_n \\ (1-\varepsilon_n)b+p_n & (1-\varepsilon_e)b_{x1} & -(1+b+b_{x1}+p'_e+p_n) & 1-\varepsilon_e+p'_e \\ b_{x2} & (1-\varepsilon_n)b+p'_n & 1+p'_e & -\{(1-\varepsilon_e)(1+b_{x2}) + b + p'_e + p'_n\} \end{bmatrix}$$

(2.3.68)

$$C_{HE} = \frac{b'}{2}\begin{bmatrix} -1 & 1 & 1 & -1 \\ 1 & -1 & -1 & 1 \\ 1 & -1 & -1 & 1 \\ -1 & 1 & 1 & -1 \end{bmatrix} \tag{2.3.69}$$

e) Difference in Spin Population Number

Substituting Eq. (2.3.61) to Eq. (2.3.66), We obtain a simultaneous equation, from which the difference in population number n, n_{34} and n_{13} can be expressed by various transition probabilities and the equilibrium value of n, n_0 .

$$\begin{bmatrix} 1+b'/2+p_e & b_{x2}-b'/2 & b+b_{x2}+p_n \\ -(1+b+b_{x1}+b'/2+p_e+p'_n) & b+b'/2+p'_n & b+b_{x1}+p'_n \\ b_{x1}-b'/2 & 1+b'/2+p'_e-(b+b_{x1}+p_n) & \end{bmatrix}\begin{bmatrix} n \\ n_{34} \\ n_{13} \end{bmatrix}$$

$$= \begin{bmatrix} -b\varepsilon_n + (1+b_{x2})\varepsilon_e \\ -b\varepsilon_n - (1+b_{x1})\varepsilon_e \\ b\varepsilon_n + (1+b_{x1})\varepsilon_e \end{bmatrix} N/4, \tag{2.3.70}$$

Note that if we observe EPR , we can set $\varepsilon_n = 0$, with $\varepsilon_e \; N/4 = n_0$. The above formula represents the most general expression for EPDR:

1) $\rho'_e = \rho_n = \rho'_n = 0$, ρ_e observed: EPR

2) $\rho'_e = \rho'_n = 0$, ρ_e observed: ENDOR

(Complete hyperfine separation)

3) $\rho'_n = 0$, ρ'_e exists, ρ_e observed: ENDOR

(Incomplete hyperfine separation)

4) $\rho_n = \rho'_n = 0$, ρ'_e pumped, ρ_e observed: ELDOR

5) $\rho_e = \rho'_e = 0$, ρ'_n pumped, ρ_n observed: Spin decoupling

6) $\rho'_e = \rho'_n = 0$, ρ_e pumped, ρ_n observed: NEDOR

In the following, we set

$$A = (1 + b + b')\{2b + (b_{x1} + b_{x2})(1 + b) + 2b_{x1}b_{x2}\}$$

$$B = 2b + (b_{x1} + b_{x2})(1 + b) + 2b_{x1}b_{x2}$$

$$C = (1 + b_{x1})(1 + b_{x2}) + (2 + b_{x1} + b_{x2})(b + \frac{b'}{2})$$

$$D = 1 + b_{x1}$$

$$E = 1 + b_{x2} \qquad (2.3.71)$$

$$F = 2 + b_{x1} + b_{x2}$$

$$G = (b + b_{x1})(b + b_{x2}) + (2b + b_{x1} + b_{x2})(1 + \frac{b'}{2})$$

$$H = 2b + b_{x1} + b_{x2}$$

$$I = 1 + b + b_{x2} + \frac{b'}{2}$$

$$J = 1 + b + b_{x1} + \frac{b'}{2}$$

Then

$$n = \frac{Y}{Z} n_0 \tag{2.3.72}$$

$$Y = A + Bp'_e + C(p_n + p'_n) + (Dp_n + Ep'_n)p'_e + Fp_n p'_n \tag{2.3.73}$$

$$\begin{aligned} Z = {} & A + G(p_e + p'_e) + C(p_n + p'_n) \\ & + Hp_e p'_e + Fp_n p'_n + I(p_n p_e + p'_n p'_e) \\ & + J(p'_n p_e + p_n p'_e) + p_e p'_e (p_n + p'_n) \\ & + p_n p'_n (p_e + p'_e) \end{aligned} \tag{2.3.74}$$

f) ENDOR Enhancement (System with Completely Separated Hyperfine)

We have

$$n = \frac{A + Cp_n}{A + Gp_e + Cp_n + Ip_n p_e} n_0 \tag{2.3.75}$$

Substituting to Eqs. (2.3.35) and (2.3.36), we obtain a similar equation to Eq. (2.3.50):

$$I = \frac{1}{2} \chi_0 B_0 \frac{\gamma_e B_1 T_{2e}}{1 + T_{2e}^2 (\omega_{e0} - \omega_e)^2 + \gamma_e^2 B_1^2 T_{1e}(\mathrm{ON})\, T_{2e}}, \tag{2.3.76}$$

where $T_{1e}(\mathrm{ON})$ is, in this case, the effective longitudinal relaxation time of an electron spin under NMR excitation:

$$T_{1e}(\mathrm{ON}) = \frac{1}{2W_e}\frac{G + lp_n}{A + Cp_n} \tag{2.3.77}$$

Note that if all relaxation paths are cut off except for W_e, *i. e.,* if $W_n = W_{x1} = W_{x2} = \omega_{HE} = 0$, we have $T_{1e}(\mathrm{ON}) = T_{1e}(\mathrm{OFF}) = \frac{1}{2}W_e$.

Thus we obtain the following expressions from Eqs. (2.3.37) - (2.3.39), corresponding to Eqs (2.2.10) and (2.2.11):

$$I_{EPR} = \frac{3\sqrt{3}}{16}\chi_0 B_0 \frac{\gamma_e B_1 T_{2e}^2}{(1 + \gamma_e^2 B_1^2 T_{1e}(\mathrm{ON})\, T_{2e})^{3/2}}, \tag{2.3.78}$$

$$I_{ENDOR} = \frac{9\sqrt{3}}{32}\chi_0 B_0 \frac{\gamma_e^3 B_1^3 T_{2e}^3 \Delta T_{1e}}{(1 + \gamma_e^2 B_1^2 T_{1e}(\mathrm{ON})\, T_{2e})^{5/2}}, \tag{2.3.79}$$

$$E = \frac{3}{2}\frac{\gamma_e^2 B_1^2 \Delta T_{1e}\, T_{2e}}{1 + \gamma_e^2 B_1^2 T_{1e}(\mathrm{ON})\, T_{2e}}, \tag{2.3.80}$$

where

$$\Delta T_{1e} = T_{1e}(\mathrm{OFF}) - T_{1e}(\mathrm{ON}) . \tag{2.3.81}$$

If $p_e >> 1$ so that $\gamma_e^2 B_1^2 T_{1e} T_{2e} >> 1$, then

$$E_\infty = \frac{3}{2}\Delta T_{1e} / T_{1e}(\mathrm{ON}) = E_{\infty\infty}\frac{p_n}{p_n + \frac{A}{C}} \tag{2.3.82}$$

where

$$E_{\infty\infty} = \frac{3}{2}\frac{\{(1+b_{x1})\,b + \frac{1}{2}b'(b_{x1}-b_{x2}) + b_{x1}(1+b_{x2})\}^2}{(1+b+b')(1+b+b_{x2}+\frac{1}{2}b')\{(2+b_{x1}+b_{x2})\,b + b_{x1}+b_{x2}+2b_{x1}b_{x2}\}} \tag{2.3.83}$$

Eqs. (2.3.80) and (2.3.82) justifies the conventional interpretation for ENDOR that it observes the variation in the longitudinal relaxation time of an electron spin by the NMR excitation. Substitution of Eq. (2.3.27) to Eq. (2.3.82) again gives a saturated Lorentzian form for the NMR transition,

$$E_{\infty} = E_{\infty\infty} \frac{\gamma_n B_2 T_{2e}}{1 + T_{2n}^2 (\omega_{n0} - \omega_n)^2 + \gamma_n^2 B_2^2 T_{1n}(\mathrm{ON})\, T_{2n}} . \quad (2.3.84)$$

with the longitudinal relaxation time of a proton,

$$T_{1n} = \frac{1}{2W_n} \frac{C}{A} \quad (2.3.85)$$

Note that if all the electron spin relaxation pathways, $W^{(e)} = 0$, then

$$T_{1n} = \frac{1}{2W_n} . \quad (2.3.86)$$

Now We can offer more simple and straightforward method to describe the fractional ENDOR enhancement, if we are interested only in its magnitude but not in its line shape. Considering from Eq. (2.3.35) that the energy absorbed by the system is simply proportional to the difference in the spin population number between which EPR is observed, the fractional ENDOR enhancement may be expressed as

$$E = \frac{n(\mathrm{ON}) - n(\mathrm{OFF})}{n(\mathrm{OFF})} , \quad (2.3.87)$$

where ON means the presence of rf field and OFF means its absence. Here we write the expression including p'_e for later discussion. Using the notation of Eqs. (2.3.71), we have

$$n(\mathrm{ON}) = \frac{(A+Bp'_e)+(C+Dp'_e)p_n}{(A+Bp'_e)+(G+Hp'_e)p_e+(C+Jp'_e)p_n+(I+p'_e)p_np_e}n_0\,, \tag{2.3.88}$$

Then the fractional ENDOR enhancement is expressed by

$$E = \frac{U-V}{V}\,, \tag{2.3.89}$$

where

$$U = \{(A+Bp'_e)+(C+DP'_e)p_n\}\{(A+Gp_e) + (G+HP'_e)p_e\} \tag{2.3.90}$$

$$V = (A+Bp'_e)\{(A+Gp_e)+(G+HP'_e)p_e + (C+Jp'_e)p_n+(I+p'_e)p_np_e\} \tag{2.3.91}$$

Setting $p'_e = 0$, we obtain the fractional ENDOR enhancement when $p_e >> 1$ and $p_n >> 1$ as

$$E_{\infty\infty} = \frac{\{(1+b_{x1})b+\frac{1}{2}b'(b_{x1}-b_{x2})+b_{x1}(1+b_{x2})\}^2}{(1+b+b')(1+b+b_{x2}+\frac{1}{2}b')\{(2+b_{x1}+b_{x2})b+b_{x1}+b_{x2}+2b_{x1}b_{x2}\}} \tag{2.3.92}$$

This is the same as Eq. (2.3.83) except for a trivial numerical factor, $\frac{3}{2}$, resulting from differentiation. In the following, we list up formula for some cases:

(i) Electron Nuclear Dipolar Mechanism ($b_{x1} = b_{x2} = b' = 0$)

$$E_{\infty\infty} = \frac{b}{2(1+b)^2} \tag{2.3.93}$$

(ii) Isotopic Hyperfine Modulation Mechanism ($b = b_{x2} = b' = 0$)

$$E_{\infty\infty} = b_{x1} \tag{2.3.94}$$

(iii) END plus Heisenberg Exchange Mechanism ($b_{x1} = b_{x2} = 0$)

$$E_{\infty\infty} = \frac{b}{2(1 + b + b')(1 + b + \frac{1}{2}b')} \tag{2.3.95}$$

The above formulas indicates that Heisenberg exchange decreases the fractional ENDOR enhancement.

(iv) END plus Cross Relaxations ($b' = 0$)

$$E_{\infty\infty} = \frac{\{(1 + b_{x1})b + b_{x1}(1 + b_{x2})\}^2}{(1 + b)(1 + b + b_{x2})\{(2 + b_{x1} + b_{x2})b + b_{x1} + b_{x2} + 2b_{x1}b_{x2}\}} \tag{2.3.96}$$

g) Comparison with Freed's Theory

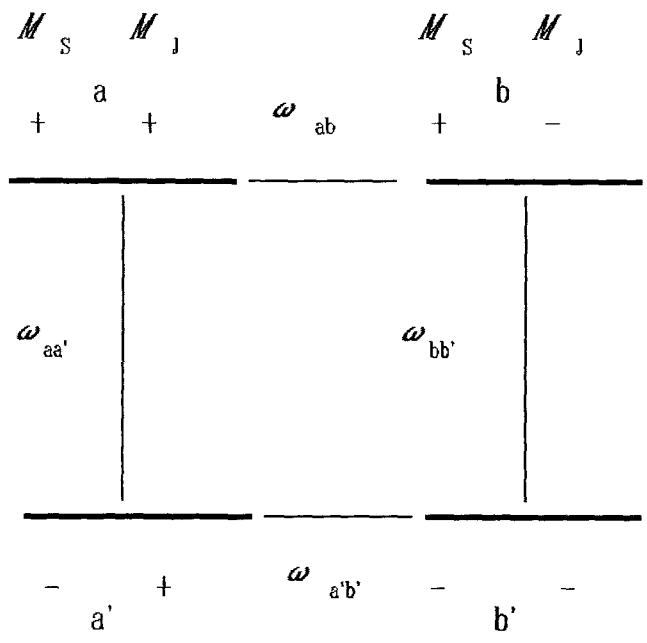

Fig. 2.4 Transitions and eigenstates for a radical with $S = 1/2$ and $J = 1/2$

We show here that the spin population number method described above for a four-level system may be regarded as the simplified version of the relaxation matrix theory developed by Freed. According to the Freed theory for a four-level system,[4,5] as illustrated in Fig. 2.4, in the case that the hf is assumed to be completely separated, the equation of motion of the density matrix is given by

$$\dot{\sigma} = -\mathrm{i}\,[\mathcal{H}_0 + \varepsilon(t),\ \sigma] - \Gamma(\sigma - \sigma_0)\ , \tag{2.3.97}$$

where σ_0 is the equilibrium density matrix, $\Gamma(\sigma - \sigma_0)$ is the relaxation matrix, and $\varepsilon(t)$ is the interaction of the spins with the oscillating magnetic field which is represented in the present case by

$$\begin{aligned}\varepsilon(t) = {} & \frac{1}{2}\gamma_e \mathcal{B}_1\{\mathcal{S}^+ \exp(-\mathrm{i}\,\omega_e t) + \mathcal{S}^- \exp(+\mathrm{i}\,\omega_e t)\} \\ & + \frac{1}{2}\gamma_n \mathcal{B}_2\{\mathcal{J}^+ \exp(-\mathrm{i}\,\omega_n t) + \mathcal{J}^- \exp(+\mathrm{i}\,\omega_n t)\}\ ,\end{aligned} \tag{2.3.98}$$

where we neglected the coupling between the $\mathcal{B}_2$ field and the electron spins as well as the $\mathcal{B}_1$ field and the nuclear spins. The former case is known to bring on so called the hyperfine enhancement effect.[18] Setting the deviation of the density matrix from its thermal equilibrium value as

$$\chi = \sigma - \sigma_0 \tag{2.3.99}$$

and denoting the steady state matrix elements of χ by $\mathcal{Z}$:

$$\chi_{ij} = \mathcal{Z}_{ij} \exp(\mathrm{i}\,\omega_{ij}\, t) \tag{2.3.100}$$

we obtain a series of equations as the off-diagonal elements of Eq. (2.3.97) at near EPR and NMR resonances:

$$\{(\omega_e - \omega_{e0}) - \frac{i}{T_{2e}}\} Z_{aa'} + d_e(x_{aa} - x_{a'a'}) + d_n Z_{b'a} = q\omega_e d_e \qquad (2.3.101)$$

$$\{(\omega_n - \omega_{n0}) - \frac{i}{T_{2n}}\} Z_{a'b'} + d_n(x_{a'a'} - x_{b'b'}) - d_e Z_{b'a} = q\omega_n d_n \qquad (2..3.102)$$

$$\{(\omega_e - \omega_{e0}) + (\omega_n - \omega_{n0}) - i/T_{b'a}\} Z_{b'a} - d_e Z_{b'a} + d_n Z_{aa'} = 0 \qquad (2.3.103)$$

Also we have the diagonal elements of Eq. (2.3.97) as follows:

$$\sum_{a \neq a'} W_{aa}(x_{aa} - x_{aa}) = 2 d_e Z''_{a'a} \qquad (2.3.104)$$

$$\sum_{a \neq a'} W_{a'a}(x_{a'a'} - x_{aa}) = -2 d_e Z''_{a'a} + 2 d_n Z''_{b'a'} \qquad (2.3.105)$$

$$\sum_{a \neq b} W_{ba}(x_{bb} - x_{aa}) = 0 \qquad (2.3.106)$$

$$\sum_{a \neq b'} W_{b'a}(x_{b'b'} - x_{aa}) = -2 d_n Z''_{b'a'} \qquad (2.3.107)$$

where the notation used are given by

$$\frac{1}{T_{2e}} = R_{aa'aa'}, \frac{1}{T_{2n}} = R_{a'b'a'b'}, \frac{1}{T_{b'a}} = R_{b'ab'a}, \qquad (2.3.108)$$

$$\omega_{e0} = \omega_{aa'}, \omega_{n0} = \omega_{a'b'}, \qquad (2.3.109)$$

$$d_e = \frac{\gamma_e B_1}{2}, d_n = \frac{\gamma_n B_2}{2}, \qquad (2.3.110)$$

and

$$q = \frac{\hbar \omega}{4kT} \qquad (2.3.111)$$

If we obtain from the above equations a solution, Z'' which denotes the

imaginary part of $\mathcal{Z}_{a'a}$, we can calculate the fractional ENDOR enhancement by

$$E = \frac{\mathcal{Z}''(\mathrm{ON}) - \mathcal{Z}''(\mathrm{OFF})}{\mathcal{Z}''(\mathrm{OFF})} \tag{2.3.112}$$

This corresponds to Eq. (2.3.87) in our theory.

It is a very tedious work to solve the series of Eqs. (2.3.101) -(2.3.107) for general case in the exact form. Instead, we can devise approximately an iterating method:

First, we suppose the case that not so large B_1 and B_2 fields are irradiated as to allow the neglecting of coherence effect,[6] as the usual condition of ENDOR measurement is so. This means the neglection of Eq. (2.3.103) as well as $\mathcal{Z}_{b'a}$ terms in Eqs. (2.3.101) and (2.3.102).

Second, we tentatively neglect the second terms in Eqs. (2.3.101) and (2.3.102). Then we obtain a Lorentzian form for $\mathcal{Z}''_{a'a}$ and $\mathcal{Z}''_{a'b'}$ which correspond to Eqs. (2.3.26) and (2.3.27) in our theory.

Third, we substitute $\mathcal{Z}''_{a'a}$ and $\mathcal{Z}''_{a'b'}$ into Eqs. (2.3.104)-(2.3.107). The equations, thus obtained, just correspond to Eq. (2.3.30).

Fourth, we calculate $\chi_{aa} - \chi_{a'a'}$ from these equations, and finally, substitute this to Eq. (2.3.101) in the exact form and then we obtain the fractional ENDOR enhancement according to Eq. (2.3.112). The procedure again corresponds to Eqs. (2.3.72) and (2.3.87).

The above procedures certainly correspond to the approach in the present theory, and so we may conclude the present theory to be the simplified version of the relaxation matrix theory developed by Freed, in the case that the B_1 and B_2 fields are not so large as to allow the above iteration method.

h) Effect of Incomplete Hyperfine Separation

In the Freed theory summarized in the previous section, it is assumed that the hyperfine splittings, $\Delta\omega$, are enough large that they are completely separated *i. e.,*

$$|\gamma_e B_1|, |\gamma_n B_2|, |R| << |\Delta\omega| \tag{2.3.113}$$

are assumed for obtaining more simple expressions. If this condition is not satisfied, we must explicitly take into consideration of the effect of the incomplete hyperfine separation.

The Allendoerfer and Maki's treatment on the effect of the incomplete hf separation has already been described in Sec. 2.2 .

In the present theory, we express this effect by the overlapping among the mw-induce transition probabilities, corresponding to the neighboring

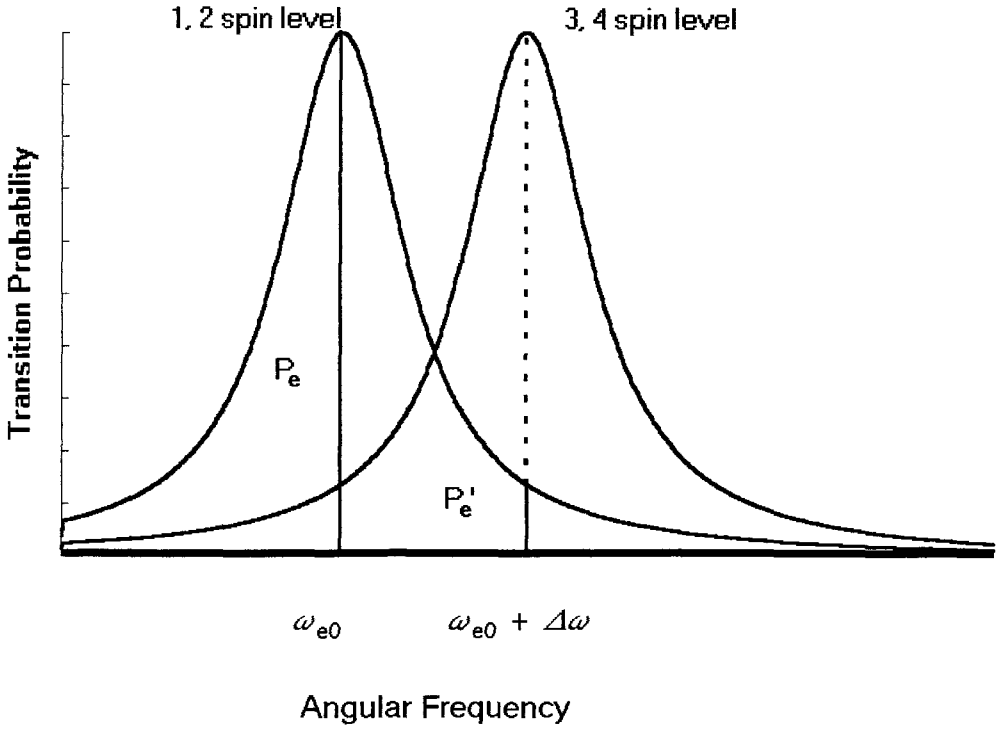

Fig. 2.5 The Effect of Incomplete Hyperfine Separation

absorption lines. As illustrated in Fig. 2.5, mw irradiation induces the transition between the observing spin levels at the EPR resonance, with probability

$$P_e = \frac{1}{2}\gamma_e^2 B_1^2 T_{2e} \tag{2.3.114}$$

At the same time, another transition probability is induced between the neighboring spin levels, with probability,

$$P'_e = \frac{1}{2}\gamma_e^2 B_1^2 T_{2e} \frac{1}{1 + T_{2e}^2 \Delta\omega^2} . \tag{2.3.115}$$

Therefore we introduce a convenient parameter, the coefficient of the incomplete hf separation, as follows:

$$\alpha = \frac{1}{1 + T_{2e}^2 \Delta\omega} . \tag{2.3.116}$$

α takes any value between 0 and 1, corresponding to the complete hf separation and the complete overlap ($\Delta\omega = 0$). Then,

$$P'_e = \alpha P_e , \quad p'_e = \alpha p_e . \tag{2.3.117}$$

i) ENDOR Enhancement (System with Incompletely Separated Hyperfine)

In the present section we examine the effect of incomplete hyperfine separation along the present scheme, in the case that the electron-nuclear-dipolar mechanism is only significant one, for the sake of simplicity, although the discussion is readily extended to more general assess. Now substituting Eq. (2.3.117) to Eq. (2.3.72) leads to formulation of the fractional ENDOR

enhancement, Eq. (2.3.87), as follows:

$$E = (1-\alpha)\frac{K}{L} \tag{2.3.118}$$

$$K = b(1+\alpha p_e)p_n p_e \tag{2.3.119}$$

$$L = 2(1+b+\alpha p_e)\{2(1+b)+(1+\alpha)(2+b)p_e+2\alpha p_e^2\}b + \{1+2b+(1+b)(1+\alpha)p_e+\alpha p_e^2\}p_n \tag{2.3.120}$$

For further analysis, the reciprocal of this equation is expanded to the first order in p_e, thus

$$\frac{1}{E} = \frac{2}{(1-\alpha)bp_n p_e}[(1+b)\{2b(1+b)+(1+2b)p_n\}+b\{(1+b)(2+b) + \alpha(2+b-b^2)\}p_e+\{(1+b)^2+\alpha(1+b-b^2)\}p_n p_e+\alpha O(p_e^2)] \tag{2.3.121}$$

Hence we obtain a straight line in plotting E^{-1} vs. p_e^{-1}, in the region where we can neglect the quadratic terms for p_e which can be proven to be proportional to α. The reciprocal of the intercept in this plot corresponds to the fractional ENDOR enhancement at infinite mw power:

$$E_\infty = \frac{1-\alpha}{2}\frac{bp_n}{\{(1+b)(2+b)+\alpha(2+b-b^2)\}b+\{(1+b)^2+\alpha(1+b-b^2)\}p_n} \tag{2.3.122}$$

Also the intercept divided by the slope of this plot is proportional to the effective longitudinal relaxation time, given by

$$T_{1e}(ON) = \frac{1}{2W_e}\frac{\{(1+b)(2+b)+\alpha(2+b-b^2)\}b+\{(1+b)^2+\alpha(1+b-b^2)\}p_n}{(1+b)\{2b(1+b)+(1+2b)p_n\}} \tag{2.3.123}$$

In addition, we obtain a saturated Lorentzian also for the NMR transition by substitution of Eq. (2.3.27) into Eq. (2.3.122), with

$$T_{1n} = \frac{1}{2W_n} \frac{(1+b)^2 + \alpha(1+b-b^2)}{(1+b)(2+b) + \alpha(2+b-b^2)} \qquad (2.3.124)$$

Then the plot of E^{-1} vs ρ_n^{-1} again gives a straight line.

j) Compromised Formula

Eq. (2.3.118) as well as Eq. (2.3.122) is still of too complicated a form for practical use. We may generally consider that a proton with a small hfs (or large α) has a small END term (or small b) and *vice versa*, as deduced from the McConell-Strathdee formula.[19] If $b << 1$, the linear part of Eq. (2.3.121) can be written as

$$E = r_H \frac{b\rho_n}{2(2b+\rho_n)}, \qquad (2.3.125)$$

where

$$r_H = \frac{(1-\alpha)\rho_e}{1+(1+\alpha)\rho_e} \qquad (2.3.126)$$

is the reduction factor due to the effect of incomplete hfs separation. By Eq. (2.3.78), I_{EPR} is optimized when $\rho_e = 1/2$. Also from Eq. (2.3.79), I_{ENDOR} is optimized when $\rho_e = 3/2$. Recalling Eq. (2.3.116), the above equation indicates that the effect of incomplete hyperfine separation reduces the fractional ENDOR enhancement by the following factors, depending on the value of ρ_e:

(i) For small ρ_e

$$r_H = \frac{T_{2e}^2 \Delta\omega^2}{1 + T_{2e}^2 \Delta\omega^2} \tag{2.3.127}$$

(ii) At the EPR maximum (ρ_e = 1/2)

$$r_H = \frac{T_{2e}^2 \Delta\omega^2}{4/3 + T_{2e}^2 \Delta\omega^2} \cdot \tag{2.3.128}$$

(iii) At the ENDOR maximum (ρ_e = 3/2)

$$r_H = \frac{T_{2e}^2 \Delta\omega^2}{8/5 + T_{2e}^2 \Delta\omega^2} \cdot \tag{2.3.129}$$

(IV) At very large ρ_e

$$r_H = \frac{T_{2e}^2 \Delta\omega^2}{2 + T_{2e}^2 \Delta\omega^2} \cdot \tag{2.3.130}$$

Therefore the numerical constant, 2.5, of the Allendoerfer-Maki factor in Eq. (2.2.15) should be replaced by 1.6 at the mw power which optimizes ENDOR enhancement. However, from the experimental viewpoint, the ENDOR enhancement is usually expected to be of best S/N ratio at the mw power which optimize the EPR intensity, and so the constant, 1.3 is recommended at this EPR power.

Next, if α = 0, Eq. (2.3.116) is written as

$$E^{(0)} = \frac{1}{2} \frac{b\rho_n}{b(1+b)(1+2b) + (1+b)^2\rho_n} \tag{2.3.131}$$

which coincides with the result of Freed equation. This equation, of course coincides with Eq (2.3.93) if ρ_n is set infinity. Therefore, from the inspection of the above two equations, it may be allowed to express

approximately the fractional ENDOR enhancement as a compromised formula including the correlation of modified Allendoerfer-Maki type and the Freed formula for b << 1, thus

$$E = r_H \; E^{(0)} . \tag{2.3.132}$$

Even under a very extreme condition that $\alpha = 1$ and $b = 1$, the deviation of Eq (2.3.132) from the linear part of Eq. (2.3.121) falls within 6 %. It decreases as b or α decreases.

k) ELDOR Reduction

In the present theory, we can calculate ELDOR reduction for a four-level system using Eqs. (2.3.72) - (2.3.74). In this case, $p_n = p'_n = 0$, and $p_o = p_e$ is the transition probability in unit of W_e, induced by mw field of the observing mode, given by

$$p_o = \frac{1}{2}\gamma_e^2 B_o^2 T_{2e} \frac{1}{1 + T_{2e}^2 (\omega_o - \omega_{o0})^2} \tag{2.3.133}$$

Also, $p_p = p'_e$ is that induced by the pumping mode mw, given by

$$p_p = \frac{1}{2}\gamma_e^2 B_p^2 T_{2e} \frac{1}{1 + T_{2e}^2 (\omega_p - \omega_{p0})^2} \tag{2.3.134}$$

Then we have from Eq. (2.3.72)

$$n\,(\mathrm{ON}) = \frac{A + B p_p}{A + G(p_o + p_p) + H p_o p_p} n_0 \tag{2.3.135}$$

where ON denotes that the mw power of pumping mode is irradiated. Thus,

we can discuss the EPR line shape exerted by the ELDOR effect by an ELDOR analogue of Eq. (2.3.76), along to the same line as the scheme in 2.3 .5 *f)* :

$$I = \frac{1}{2}\chi_0 B_0 \frac{\gamma_e B_0 T_{2e}}{1 + T_{2e}^2 (\omega_{00} - \omega_0)^2 + \gamma_e^2 B_1^2 T_{1e} T_{2e}} \quad (2.3.136)$$

where

$$T_{1e}(\mathrm{ON}) = \frac{1}{2W_e}\frac{G + Hp_p}{A + Gp_p}. \quad (2.3.137)$$

These equation indicate that the ELDOR phenomena can be again understood by the change in the effective longitudinal relaxation time of an electron spin, arising from the irradiation of the pumping mw field. Here we employ the similar definition to Eq. (2.3.87) for the fractional ELDOR reduction:

$$R = \frac{n(\mathrm{OFF}) - n(\mathrm{ON})}{n(\mathrm{OFF})}. \quad (2.3.138)$$

Then substituting Eq. (2.3.135), we obtain

$$R = \frac{\{A(G - B) + (AH - BG)p_0\}p_p}{A\{(A + Gp_0) + (G + Hp_0)p_p\}} \quad (2.3.139)$$

Therefore the fractional ELDOR reduction is expressed as the saturated Lorentzian form in regard to p_p as well as p_0. Usually, EPR is monitored by use of the very weak observing power that $p_0 << 1$. Under such condition, the above equation is simplified to

$$R = \frac{(G - B)p_p}{A + Gp_p} \quad (2.3.140)$$

Thus, we obtain an ultimate expression at infinite pumping powe as

$$R_\infty = \frac{b^2 - b_{x1}\, b_{x2} + \frac{1}{2}b'(2b + b_{x1} + b_{x2})}{(b + b_{x1})(b + b_{x2}) + (1 + \frac{1}{2}b')(2b + b_{x1} + b_{x2})} \tag{2.3.141}$$

This corresponds to the reciprocal of the intercept of the straight line in plotting R^{-1} *vs.* p_p^{-1}. Also,

$$T_{1o} = \frac{1}{2W_e}\frac{G}{A} = \frac{(1+b+b')\{b+(b_{x1}+b_{x2})(1+b)+2b_{x1}\, b_{x2}\}}{(b+b_{x1})(b+b_{x2})+(1+\frac{1}{2}b')(2b+b_{x1}+b_{x2})}\frac{1}{2W_e} \tag{2.3.142}$$

corresponding to the effective longitudinal relaxation time of the pumping mode absorption, which is proportional to the ratio of the intercept divided by the slope of the plot mentioned above. We write here the limiting formula of Eq. (2.3.141) in some cases:

(i) END Mechanism ($b_{x1} = b_{x2} = b' = 0$)

$$R_\infty = \frac{b}{2 + b} \tag{2.3.143}$$

(ii) END plus Heisenberg exchange mechanism ($b_{x1} = b_{x2} = 0$)

$$R_\infty = \frac{b + b'}{2 + b + b'} \tag{2.3.144}$$

(iii) END plus cross relaxations mechanism ($b' = 0$)

$$R_\infty = \frac{b^2 - b_{x1}\, b_{x2}}{(b + b_{x1})(b + b_{x2}) + 2b + b_{x1} + b_{x2}} \tag{2.3.145}$$

In this case, if cross relaxations are predominant to END terms, we can expect the ELDOR enhancement, as experimentally detected.[21,22]

2.3.6 ENDOR Enhancement for a Multi-Level System - a Simplified Method

a) Formulation

So far we considered a radical which has only one proton. However, most radicals have several sets of equivalent protons or in some cases, nitrogens. Their EPR absorption line is formed by the superposition of their component lines, each designated by the various quantum numbers of the total nuclear spin angular momentum. Therefore, for the quantitative discussion of the ENDOR relaxation, we must proceed to a multi-level system, consisting of several sets of equivalent protons. Treatment of this system along the same lines as the scheme in previous section may be possible, in principle, but it requires too complicated and tedious processes and deviates from the purpose of the present study. Instead, a simplified method of calculating the fractional ENDOR enhancement for such a system is proposed with the following approximation and derivations:

In a multi-level system,[20] the spin state is represented by

$$| \gamma^{\pm} \rangle = | \pm\frac{1}{2} \rangle \prod_{u} | J_u^{(k)}, M_u \rangle \quad , \tag{3.2.146}$$

where J_u and M_u are the quantum number of the total nuclear spin angular momentum for the u'Th set of equivalent protons with M_u as the z

-component of J_u, and k denotes the different degenerate states with the same value of J_u.

Now we first assume that T_{2e} is independent of J_u and M_u, so that the EPR absorption is expressed as the superposition of component lines having the same line width, corresponding to the transitions from $|\gamma^-\rangle$ to $|\gamma^+\rangle$. On the other hand, the nuclear spin transition probabilities are assumed to depend on the nuclear spin quantum numbers, as follows:[5]

$$\frac{1}{T_{2n}}(J_u, M_u \Leftrightarrow J_u, M_u\text{-}1) = W_e[\ 1 + \{2f(J_u, M_u) + \frac{1}{3}\} b_u]\ , \tag{2.3.147}$$

$$W_n(J_u, M_u \Leftrightarrow J_u, M_u\text{-}1) = f(J_u, M_u)\, W_n(u) \tag{2.3.148}$$

$$P_n(J_u, M_u \Leftrightarrow J_u, M_u\text{-}1) = f(J_u, M_u)\, P_n(u) \tag{2.3.149}$$

where $W_n(u)$ and $P_n(u)$ are the nuclear spin transition probabilities induced by lattice and rf field, respectively, for a four-level system consisting of a single u's proton, with

$$f(J_u, M_u) = J_u(J_u + 1) - M_u(M_u - 1)\ , \tag{2.3.150}$$

We denote

$$b^{(u)} = \frac{W_n^{(u)}}{W_e}\ , \tag{2.3.151}$$

$$p_n^{(u)} = \frac{P_n^{(u)}}{W_e}\ . \tag{2.3.152}$$

$$f(J_u, 0 \text{ or } 1/2) = f_{J_u} \tag{2.3.153}$$

(0 : even number 1/2 : odd number of protons)

Second, we treat an enough dilute solution that the Heisenberg spin exchange effect can be neglected. Also, we assume that the END

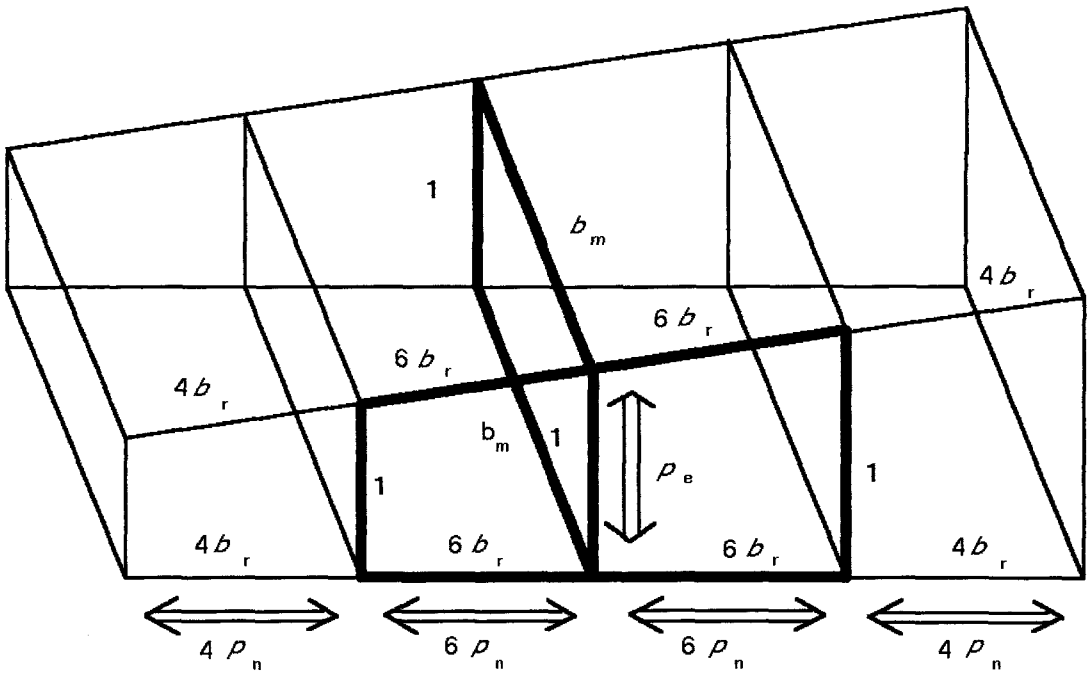

Fig. 2.6 Schematic diagram of the energy levels and the transition probabilities for a system with two kinds of one proton ($J_m = 1/2$) and four protons ($J_r = 2$). The central line of one of the quintets of doublet of EPR absorption is observed (p_e), and the rf field corresponding to the hfs of the r th equivalent protons is irradiated. The right side diagram draws an equivalent two-level system corresponding to the summation of relaxation pathways with thick line in the left diagram.

mechanism is the only significant relaxation pathways and we neglect the cross relaxations. Such condition may be well satisfied for protons in most of the organic radicals in liquid phase except for some cases in which the isotopic hyperfine modulation may be effective.

Third, we neglect the relaxation pathways passing more than twice through the W_n 's, under the assumption that $b \ll 1$. For example, for the

system with $J_m = 1/2$ and $J_r = 2$ as illustrated in Fig. 2.6, only the relaxation pathways with thick line are considered. Then all the multi-level system are reduced to the superposition of the four-level or six-level systems. This can further be reduced to the two level system illustrated in the right of Fig. 2.6 The EPR absorption for this system has already been treated in 2.3.4 and we have obtained Eq. (2.3.49) as the mw energy absorbed in unit time. This equation indicates that if mw power is enough large that $\rho_e \gg w$, the spin lattice relaxation becomes the rate-determining step of energy absorption:

$$A_\infty = n_0 \hbar\omega_e W_e , \tag{2.3.154}$$

Therefore we may define an alternative form for the fractional ENDOR enhancement when enough large mw power is employed as

$$E_\infty^{(0)} = \frac{w\,(\mathrm{ON}) - w\,(\mathrm{OFF})}{w\,(\mathrm{OFF})} \tag{2.3.155}$$

corresponding to Eq. (2.3.85), where ON and OFF means the presence and the absence of pn, and $w = W/W_e$.

For actual application, it is sufficient only to treat the central line of the EPR absorption. In this case, the summing up method leads to the following resultant transition probability for an electron spin:

$$w = 1 + \sum_u \sum_{J_u} \frac{D_{J_u}}{D_u} \frac{2 f_{J_u} b_u (b_u + \rho_n^{(u)})}{(2 + f_{J_u} b_u) b_u + (1 + f_{J_u} b_u) \rho_n^{(u)}}$$

$$+\sum_{u'}\sum_{J_{u'}}\frac{D_{J_{u'}}}{D_{u'}}\left[\frac{(f_{J_{u'}}-1)\,b_{u'}(b_{u'}+\rho_n^{(u')})}{\{2+(f_{J_{u'}}-1)\,b_{u'}\}\,b_{u'}+\{1+(f_{J_{u'}}-1)\,b_{u'}\}\rho_n^{(u')}}\right.$$

$$\left.+\frac{f_{J_{u'}}b_{u'}(b_{u'}+\rho_n^{(u')})}{(2+f_{J_{u'}}b_{u'})\,b_{u'}+(1+f_{J_{u'}}b_{u'})\rho_n^{(u')}}\right] \qquad (2.3.156)$$

where u and u' denote, respectively, even and odd number of equivalent protons, D_u is the total degeneracy of the central absorption line of u'th set of equivalent protons, and D_{J_u} is the degeneracy of the state with the same value of J_u. These are given by

$$D_{J_u}=\frac{n_u(n_u-1)\ldots([n_u/2]-J_u+1)\,(2J_u+1)}{[n_u/2]+J_u+1} \qquad (2.3.157)$$

$$D_u=\sum_{J_u}D_{J_u}=\begin{pmatrix} n_u \\ n_u/2 \end{pmatrix} \qquad (2.3.158)$$

where n_u is the number of u'th equivalent protons, and $\sum_{J_u}$ denotes the single summation over the u' th set of equivalent protons.

It can be proven that for a six-level system in the case that hfs is incompletely separated, a calculation similar to Eq. (2.3.87) leads to the same form of the fractional ENDOR enhancement as Eq. (2.3.132). Therefore, it is considered that Eq. (2.3.132) is still valid for the general multi-level systems, as long as the above approximation of treating them as the superposition of four- or six-level systems is valid. Hence, we are able to calculate the fractional ENDOR enhancement from Eqs. (2.3.132), (2.3.155),

and (2.3.154). Here we write only the limiting expressions. For very large rf power irradiated on even number of equivalent protons ($\rho_n = \infty$):

$$E,_{\infty}{}^{(u)} = r_H \sum_{J_u} \frac{D_{J_u}}{D_u} \frac{2 f_{J_u} b_u}{(1 + f_{J_u} b_u)(2 + f_{J_u} b_u)} \Big/ w(\mathrm{OFF}) \,. \tag{2.3.159}$$

For infinitesimal rf power irradiated on even number of equivalent protons ($\rho_n \ll 1$):

$$E,_0{}^{(u)} = r_H \sum_{J_u} \frac{D_{J_u}}{D_u} \frac{2 f_{J_u} \rho_n^{(u)}}{(2 + f_{J_u} b_u)^2} \Big/ w(\mathrm{OFF}) \,. \tag{2.3.160}$$

Also, for odd number of equivalent protons, we have

$$E,_{\infty}{}^{(u')} = r_H \sum_{J_{u'}} \frac{D_{J_{u'}}}{D_{u'}} \left[\frac{f_{J_{u'}}}{(1 + f_{J_{u'}} b_{u'})(2 + f_{J_{u'}} b_{u'})} + \frac{f_{J_{u'}} - 1}{\{1 + (f_{J_{u'}} - 1) b_{u'}\}\{2 + (f_{J_{u'}} - 1) b_{u'}\}} \right] b_{u'} \Big/ w(\mathrm{OFF}) \,. \tag{2.3.161}$$

For infinitesimal rf power irradiated on even number of equivalent protons ($\rho_n << 1$):

$$E,_0{}^{(u')} = r_H \sum_{J_{u'}} \frac{D_{J_{u'}}}{D_{u'}} \left[\frac{f_{J_{u'}}}{(2 + f_{J_{u'}} b_{u'})^2} \right.$$

$$+\left.\frac{f_{J_u'}-1}{\{2+(f_{J_u'}b_{u'}-1)\}^2}\right\} p_n^{(u)}/w(\mathrm{OFF}) \qquad (2.3.162)$$

In the plot of E^{-1} vs. p_n^{-1}, the reciprocal plot of the intercept is equal to the fractional ENDOR enhancement at infinite rf power which corresponds to Eqs. (2.3.159) and (2.3.161). Also, the reciprocal of the slope is proportional to that at infinitesimal rf power which corresponds to Eqs. (2.3.160) and (2.3.162). The linearity of such plots la approximately assured, because, in general, if $x \ll r_i/q_i$,

$$y=\sum_i \frac{p_i}{q_i x+r_i}=\frac{\sum_i (p_i/q_i)^2 x}{\sum_i (p_i/q_i)\,x+\sum_i (p_i r_i/q_i^2)} \qquad (2.3.163)$$

Application of Eqs. (2.3.151) and (2.3.162) to a four-level system leads, of course, to the same results as Eq. (2.3.132) with Eq. (2.3.131).

Because

$$\sum_{J_u}\frac{D_{J_u}}{D_u}=n_u/2\ , \qquad (2.3.164)$$

the above equation can further be reduced to more simplified form, if we can neglect the quadratic terms for b_u:

$$E_{,\infty}^{(u)}=r_H\frac{n_u b_u}{2}\ , \qquad (2.3.165)$$

$$E_{,0}^{(u)}=r_H\frac{n_u p_n^{(u)}}{4}\ , \qquad (2.3.166)$$

where in this case, u denotes even and odd numbers of equivalent protons. Considering that from Eq. (2.3.147), $\rho_n^{(u)}$ is independent of u if $b_u \ll 1$, we can deduce an interesting conclusion that if the hfs's are completely separated, the reciprocal of the slope in the plot of the reciprocal of the fractional ENDOR enhancement against the reciprocal of rf power is proportional to the number of equivalent protons. Similar result is also obtained from the "average ENDOR" proposed by Freed *et al.* [6] Thus, Eq. (2.3.162) reasonably offers how to examine the effect of incomplete hyperfine separation. That is, the B_2 dependence of the ENDOR enhancement is measured at high temperature of which $b_u \ll 1$ is satisfied for all protons. the reciprocal of the slope obtained from its reciprocal plot is divided by the number of equivalent protons, and then the results are compared among proton species.

Although ENDOR experiments have been reported in the literature for many radicals in liquid phase since the first successful observation by Hyde and Maki,[22] ENDOR detection for many radicals remains impossible or at least difficult, in spite of the ease of EPR observation. Perhaps, the Heisenberg and chemical exchanges are the reason. Also, Another is due to the fact that the $J = 0$ state in a multi-level system is ENDOR inactive. However, Eqs. (2.3.160) to (2.3.162) offer additional reason. In these equations, all the END terms of atoms having nuclear spins make contribution to the numerator, in contrast that only those of observing proton contribute to the denominator. Therefore if a radical contains atoms having a nuclear spin on which the electron spin density is moderately localized resulting in a large END term, we may expect only weak ENDOR enhancement. This may be a possible reason why the ENDOR

enhancement for hydrocarbon radicals is, in general, more easily observed than that for nitroxide radicals.

b) Some Remarks on TRIPLE enhancement

The TRIPLE enhancement in the EPR spectroscopy is the abbreviation of the electron-nuclear-nuclear triple enhancement. That is, we observe the EPR enhancement during the simultaneous irradiation of two kinds of rf powers. The liquid phase TRIPLE experiment was first succeeded by Mobius et al.[22] It is very useful for obtaining detailed information of a radical, such as accurate hfs constant or its sign.[23,24] The most attractive results of their first experiment are that the TRIPLE enhancement has better S/N ratio than does the ENDOR enhancement and that the TRIPLE enhancement is nearly proportional to the number of equivalent protons in a radical. The TRIPLE enhancement has been theoretically treated by Freed for a four-level system. Here we give some remarks to TRIPLE enhancement on the standpoint of the present theory.

We define the fractional TRIPLE enhancement by Eq. (2.3.87), but in this case, ON means the presence of both ρ_n and ρ'_n. Straightforward calculation, using Eqs. (2.3.72) - (2.3.74) gives the following expression to the fractional TRIPLE enhancement in the case that END terms are the only significant relaxation mechanism and that $\rho_n = \rho'_n$:

$$E_T = \frac{P}{Q} \tag{2.3.167}$$

$$P = (1 - \alpha)\rho_e \rho_n (1+\alpha\rho_e)(b+\rho_n) \tag{2.3.168}$$

$$Q = (1 + b + \alpha p_e)[\{p_n^2 + 2(1 + b + \alpha p_e)p_n + (2 + b + 2\alpha p_e)b\}p_e + (2 + \alpha p_e)p_n^2 + 2\{1 + 2b + (1 + b)\alpha p_e\}p_n + b\{2 + 2b + (2 + b)\alpha p_e\}] . \quad (2.3.169)$$

The above equation indicates, however, that the effect of the incomplete hyperfine separation also reduces the TRIPLE enhancement. Indeed, the TRIPLE enhancement for 2,6-*t*butyl protons in the 2,4,6-*tri-t*butyl phenoxyl radical[22] appears to support the presence of this effect. In addition, the above equation indicates that we may expect an eight times better S/N ratio for the TRIPLE enhancement when we compare the equation with Eq. (2.3.93) at their optimum conditions.

For a multi-level system, we start with Eq. (2.3.155) as the basis of discussion. However, because p_n and p'_n are simultaneously irradiated, even the previous approximation to reduce a multi-level systems to the superposition of four- or six-level systems is now not valid. Instead, we consider the entire system in the extreme cases that $p_n = p'_n = 0$ for the OFF state and that $p_n = p'_n = \infty$ for the ON state under the condition that $b \ll 1$. Then, in the former case, all the relaxation pathways are cut off except for the W_e's of the original two-level system, because of $b \ll 1$. In the latter case, all the W_n pathways are short-circuited by p_n and p'_n, so that the W_e pathways are gathered to form a net two-level system. Thus, we obtain

$$w(\mathrm{ON}) = \sum_{J_u} \frac{D_{J_u}}{D_u}(2J_u + 1) , \quad (2.3.170)$$

with w (OFF) = 1. Hence, from Eq. (2.3.85), the fractional TRIPLE enhancement for the u'th equivalent protons is given by

$$E_T(u) = \sum_{J_u} \frac{D_{J_u}}{D_u} 2 J_u . \qquad (2.3.171)$$

Such a simple formula appears to explain fairly well the experimental results demonstrated by Mobius et al.[22] For example, the ratio of the TRIPLE enhancement for 2,4,6,10-protons to that for 1,7-protons in the pyrene negative ion is reported to be 1.3, whereas the theoretical ratio from Eq. (2.3.171) is 1.67 which is nearer to the experimental one than the simple ratio of the number of equivalent protons, 2.

3.1 ENDOR Relaxation of Galvinoxyl

3.1.1 Introduction

A phenomenological theory for EPDR, including ENDOR, has been developed in Chapter 2. The purpose of the present chapter is to report the results of the measurement of ENDOR enhancement of galvinoxyl, focusing our attention to an experimental examination of the applicability and the limit of the present theory.

The pulse techniques which have been widespread in the field of NMR spectroscopy is more difficult in the field of EPR spectroscopy, because of much higher resonance frequency of the latter. Since the first measurement of the pulse EPR by Mims,[1] and improved measurement by Hyde *et al.*,[2] recent progress of mw techniques have enabled the measurement of EPR in the frequency domain. Nevertheless from an analysis of measurement of EPR in the field domain, such as its saturation curves and line widths,[3] it is expected that abundant experimental information about the relaxational behavior of a radical can be extracted. The similar procedure in the field domain measurement should be applicable also to ENDOR, by measuring the micro wave- (mw) and rf power dependence of ENDOR enhancement. More abundant information can be expected, because two parameters can be varied independently. Leniart *et al.*[4] have applied such a method to the

---

1 W. B. Mims, *Rev. Sci. Instrum.*, **36**, 1472 (1965).

2 M. Huisjen and J. S> Hyde, *Rev. Sci. Instrum.*, **45**, 669 (1974)

3 R. G. Kooser, W. V. Volland, and J. H. Freed, *J. Chem. Phys.*, **50**, 5243 (1969).

4 D. S. Leniart, S. D. Connor, and J. H. Freed, *J. Chem. Phys.*, **63**, 165 (1975).

study of some semiquinones. However, to the present author's knowledge, there have been no attempt to compare these dependence for different proton species in a molecule over a wide temperature range.

In the present study, the ratio of the ENDOR enhancement to the EPR intensity was measured for different protons, as function of mw and rf powers at temperature from -20 ℃ to -95 ℃. The sample used in the experiments is the galvinoxyl radical which has one methylidyne proton, four ring protons and thirty-six *t*-butyl protons. It was selected because its ENDOR spectra is one of the most easily observable and because The impurity of this very stable radical can be precisely determined from a measurement of the magnetic susceptibility, so that a solution of known concentration can be easily obtained. It is one of materials for which the liquid phase ENDOR was first successfully observed.[5] The results are discussed with reference to the theory in Chapter 2, focusing our attention on a comparison of the proton species.

3.1.2 Experimental

The ENDOR spectra were measured using a JEOL EDX-1 ENDOR unit with a frequency modulation of 6.5 kHz, attached to a JEOL ME-X EPR spectrometer with a field modulation of 80 Hz. The rf amplifier employed can provide maximum rf power of 1kW. The mw power was calibrated using the EPR intensity of powdered DPPH. The rf power was measured using a level meter connected to a tank circuit which was calibrated by a 100-MHz oscilloscope, using a search coil. No attempt was made to determine the absolute value of either magnetic field. The intensity of 80-Hz field

---

[5] J. S. Hyde and A. H. Maki, *J. Chem. Phys.*, **40**, 3117 (1964).

modulation was set to 3 db lower than that for optimum ENDOR enhancement, because over-modulation reduces the relative enhancement for *t*-butyl protons with respect to the enhancement of other protons.[6]

A toluene solution of galvinoxyl in a quartz tube was degassed by a usual method. The purity of of the compound synthesized in this laboratory in the past was determined to be 85 %. The viscosity of toluene was estimated using the empirical formula reported by Barlows et al.[7] In most of cases, the ENDOR enhancement was measured as the peak-to-peak heights of the first derivative of lines. However, because the ENDOR enhancement for the *t*-butyl proton was not completely dissolved completely at high temperatures, it was measured as the distance from the highest to the lowest peak of the doublet enhancement.

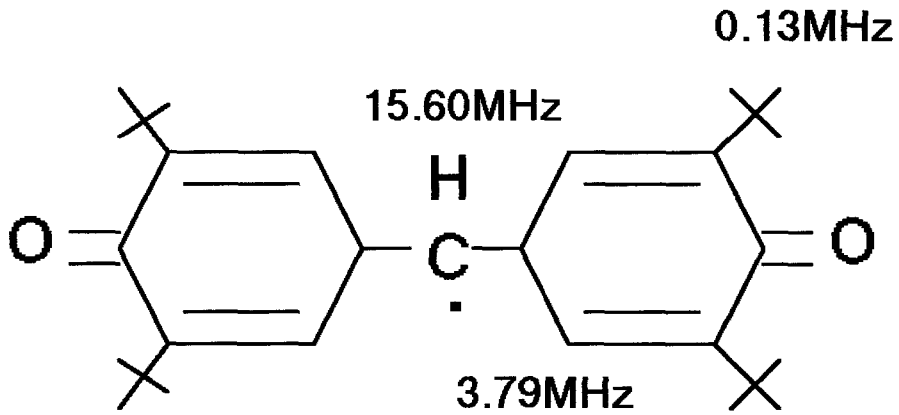

Fig. 3.1 Structure of galvinoxyl.

---

6 R. D. Allendoerfer and A. H. Maki, *J. Mag. Reson.*, 3, 396 (1970).

7 A. J. Barlow, J. Lamb, and A. J. Matheson, *Proc. Loy. Soc.*, 292, 322 (1966).

a) ENDOR Spectra of Galvinoxyl

An example of an EPR spectrum and an ENDOR enhancement of galvinoxyl (Fig. 3.1) at -80 ℃ are shown in Fig. 3.2 . For the latter

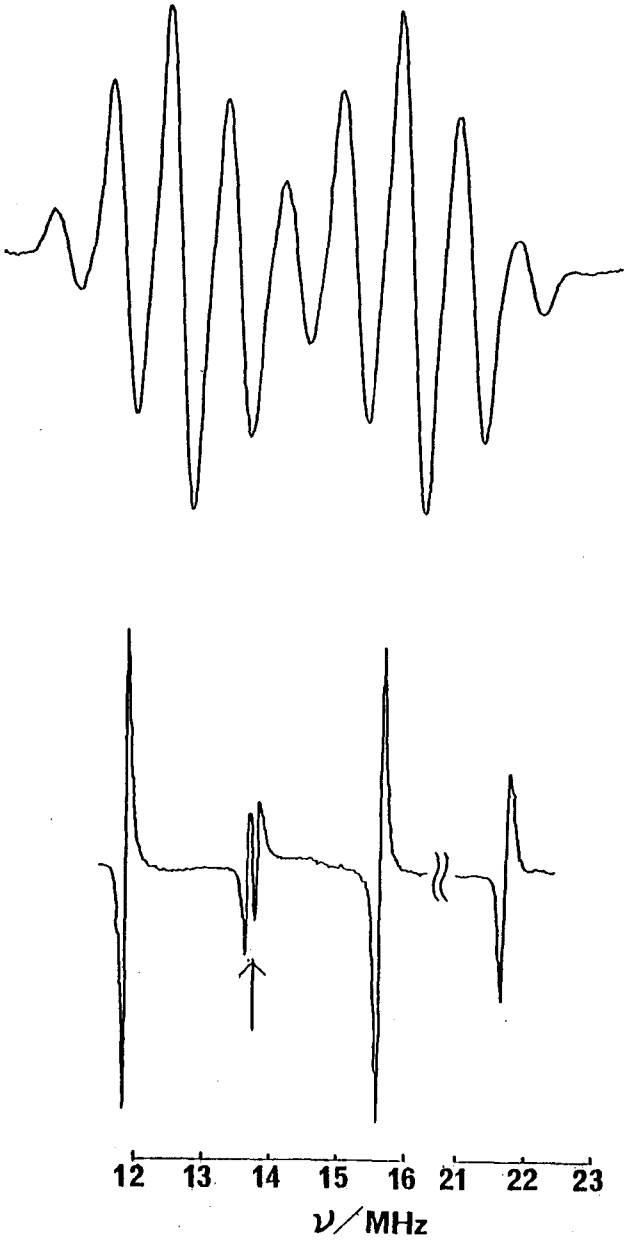

Fig. 3.2 EPR spectrum and ENDOR spectra of galvinoxyl in toluene at -80 ℃. The arrow line indicates the free proton frequency.

measurement, the EPR field was adjusted to the highest peak of the low-filed part of the doublet of the methylidyne proton. The EPR spectrum completely splits the doublet of quintets of methylidyne and ring protons, but does not resolve any *t*-butyl proton splitting. From the ENDOR spectrum, however, the hfs constants are found to be 15.60, 3.79, and 0.13 MHz at -80 ℃, corresponding to methylidyne, ring and *t*-butyl protons, respectively. No marked dependence of the hfs constants on temperature was observed. In the following discussion, the proton species in galvinoxyl are denoted by the subscripts, m, r, tb, respectively.

In the present work, the ENDOR enhancement is always divided by the EPR intensity of the peak for which the ENDOR was observed. The quantity, which we tentatively call ENDOR quotient, is taken to be proportional to the fractional ENDOR enhancement. The procedure will remove experimental errors which may result from, for example, a change in Q value of the cavity during the measurement of the mw-power, rf-power and the temperature dependence. Moreover, the ENDOR quotient is more favorable from the viewpoint of theoretical analysis.

Regarding variation of concentration, the ENDOR enhancement is optimized at about 3×10^{-4} M, and is sharply decreased for other concentrations. On the other hand, the ENDOR quotient monotonically increases and appears to approach to a limiting value. More detailed results will be discussed in a subsequent paper, and it is merely noted here that the ratio of the ENDOR enhancement for different protons at the concentration used here is almost the same as the limiting ratio. Thus, we temporarily neglect the Heisenberg exchange effect, because the addition of another ambiguous parameter would not aid in understanding the essential features of the present system. In the later sections, 3.1.4 *a)* and *b)*, we discuss the

experimental results in connection with the theory for a four-level system in Chapter 2, Sec. 2.3.5, and further, we discuss them in Sec 3.1.4 c) in comparison with the theory for a multi-level system in Chapter 2, Sec. 2.3.6.

3.1.3 Dependence on Mw Power

Fig. 3.3 shows the EPR intensity, the ENDOR enhancement and the ENDOR quotient on the mw power, measured at -75 ℃. The rf power employed is indicated by the arrowed in Fig 3.7. This figure shows that for sufficiently weak mw powers, the EPR intensity is proportional to the square

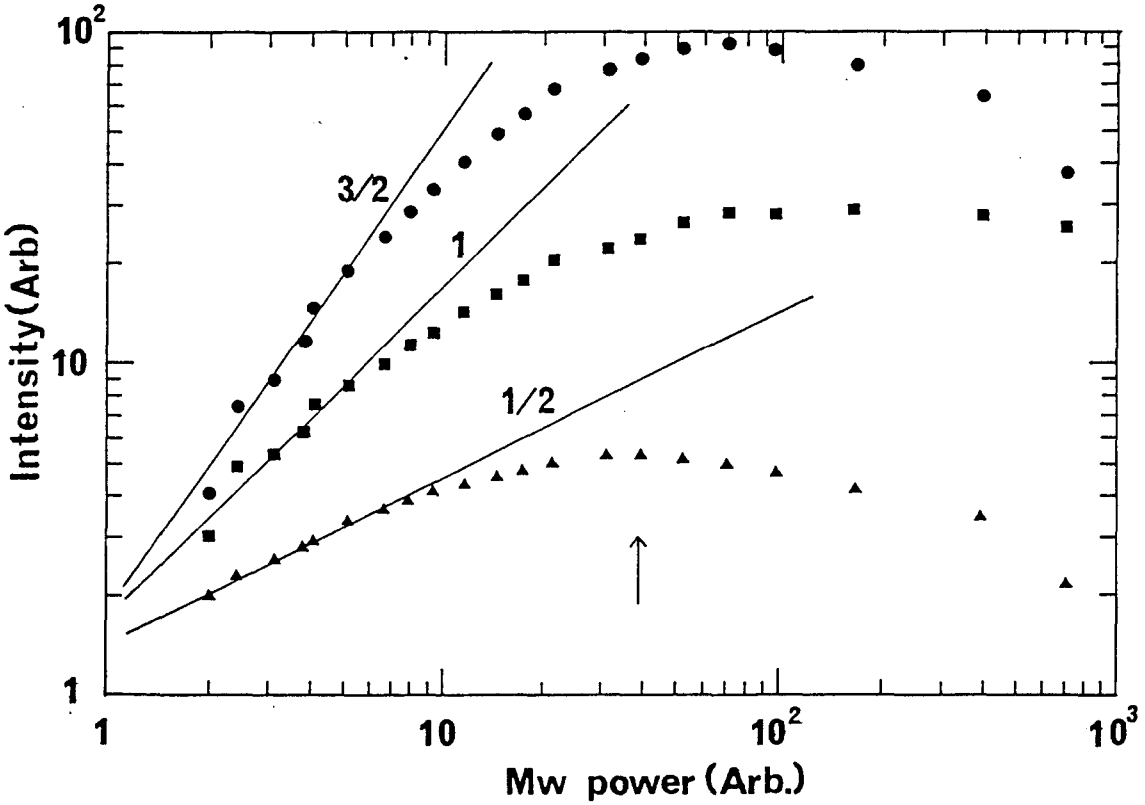

Fig. 3.3 Dependence of EPR intensity I_{EPR} (▲), ENDOR enhancement I_{ENDOR} (●) and ENDOR quotient I_{ENDOR}/I_{EPR} (■) of ring protons on mw power. The arrow indicates the mw power used for the measurement in Figs. 3.5 - 3.8. The numbers on the line indicate the order in the low-power region.

root of the mw power, the ENDOR enhancement to the 3/2 power of the mw power, so that the ENDOR quotient is simply proportional to the mw power. The fact is clearly predicted by the Equations in Chapter 2, listed again in the following;

$$I_{EPR} = \frac{3\sqrt{3}}{16} \chi_0 B_0 \frac{\gamma_e B_1 T_{2e}^2}{(1 + \gamma_e^2 B_1^2 T_{1e}(ON) T_{2e})^{3/2}} , \qquad (3.1.1)$$

$$I_{ENDOR} = \frac{9\sqrt{3}}{32} \chi_0 B_0 \frac{\gamma_e^3 B_1^3 T_{2e}^3 \Delta T_{1e}}{(1 + \gamma_e^2 B_1^2 T_{1e}(ON) T_{2e})^{5/2}} , \qquad (3.1.2)$$

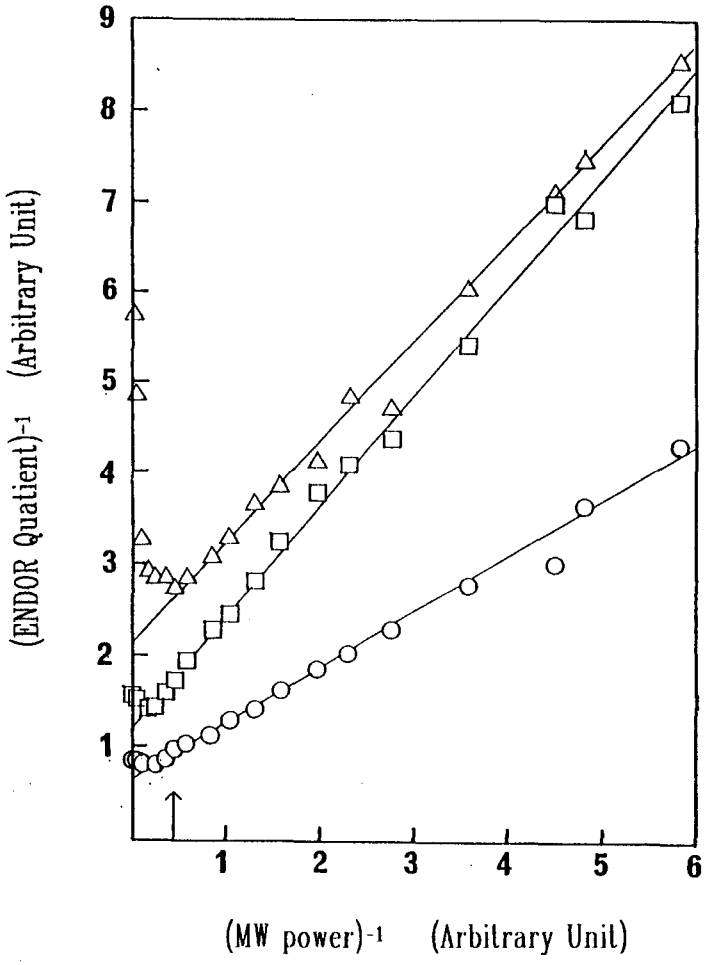

Fig. 3.4 Reciprocal of the ENDOR quotient as a function of the reciprocal of the mw power. The triangles are for *t*-butyl protons, circles for ring protons and square for a methylidyne proton. The arrow indicates the same mw power as in Fig. 3.3 .

$$E = \frac{3}{2} \frac{\gamma_e^2 B_1^2 \Delta T_{1e} T_{2e}}{1 + \gamma_e^2 B_1^2 T_{1e}(\mathrm{ON}) T_{2e}} . \qquad (3.1.3)$$

The conventional method to determine experimental relaxation time, T_{1e} has been the saturation method. From Fig. 3.3, the ratio of B_1 giving ENDOR maximum to that giving EPR maximum is proved precisely to be 3.0, both from theoretical and experimental viewpoint. Thus the ENDOR method offers another method to determine T_{1e}, in addition to the conventional EPR method, and this will to increase reliability of the saturation method to compare with T_{1e} determined directly from the time domain measurement in future.

Also, interesting features are found in Fig. 3.4, in which the reciprocal of the ENDOR quotient for different protons is plotted against the reciprocal of the mw power. As the mw power is increased over a moderately wide range, all the plots go down linearly, as is understood by Eq. (3.1.3), but they start to turn up as the mw power is further increased. This means that the ENDOR enhancement decreases more rapidly than does the EPR intensity with a further increase of the mw power. Such a tendency is most marked for *t*-butyl protons, and a more detailed examination reveals that the mw power corresponding to the point at which the plot deviates from a straight line for this proton is about one-half of those for methylidyne and ring protons. The result is considered to indicate the importance of the effect of incomplete hyperfine separation for *t*-butyl protons.

In the present theory, the effect of incomplete hf separation is parametrized by a coefficient, α, defined by

$$\alpha = \frac{1}{1 + T_{2e}^2 \Delta\omega^2} . \qquad (3.1.4)$$

where $\Delta\omega$ is the hfs constant. Considering that the EPR resolves no splitting for *t*- butyl protons in contrast to the case of methylidyne and ring protons and that T_{2e} is ordinarily has a value of 10^{-6} - 10^{-7} s, the α for galvinoxyl will be $0 \sim \alpha_m$, $\alpha_r \ll \alpha_{tb} < 1$. It is shown in the theory, that the plot of E^{-1} vs. p_e^{-1} forms a straight line in the weak mw-power region and that the deviation from linearity at higher mw power is due to the quadratic terms for p_e , which are proportional to α (Eq. (2.3.121)). Thus, the theory explains well the experimental features mentioned above, taking account of the difference in the αvalues.

Furthermore, the effective longitudinal relaxation time of an electron spin, T_{1e}, under rf-power excitation is given by

$$T_{1e}(\mathrm{ON}) = \frac{1}{2W_e} \frac{\{(1+b)(2+b)+\alpha(2+b-b^2)\}b+\{(1+b)^2+\alpha(1+b-b^2)\}p_n}{(1+b)\{2b(1+b)+(1+2b)p_n\}} \tag{3.1.5}$$

Since b is considerably smaller than 1 at temperatures normally used for ENDOR, this equation is reduced to

$$T_{1e}(\mathrm{ON}) = \begin{cases} \dfrac{1}{2W_e} & (\alpha = 0) \\ \dfrac{1}{W_e} & (\alpha = 1) \end{cases} \tag{3.1.6}$$

On the other hand, from Eq. (2.3.113), the slope divided by the intercept of the linear part of the plot in Fig. 3.4 is interpreted as being proportional to T_{1e}(ON). The their experimental ratio 1 : 1.0 : 1.9, for methylidyne, ring and *t*-butyl protons, respectively, as setting that of methylidyne proton to be 1. The good agreement between the experimental and the theoretical results suggests the validity of the treatment for the effect of incomplete hf

separation developed in Chapter 2, although coherence effect[8] may also be involved in the upward-turning tendency of the curve in the high mw-power region in Fig. 3.4 . This is beyond the limits of the present theory.

A similar situation for the mw-power saturation of ENDOR enhancement is also found for the 2,4,6-*tri-t*-butylphenoxyl radical in mineral oil,[6] where the values of the mw power for optimum ENDOR enhancement decreases in the order, 2,6-*di-t*-butyl, 4 -*t*-butyl, and 3,5- ring protons. Such a result suggests the importance of the effect of HS separation for the former two types of protons.

3.1.4 Dependence on Rf Power

During the analysis of ENDOR enhancement as a function of rf power, we must keep in mind the effect of hf enhancement.[9] In addition to the external rf field, the nuclear spin is affected by another field, caused from the rf modulation of hf coupling with the electron spin, so that if $|\Delta\omega|/2 < \omega_p$, the effective rf field is given by

$$B_{2\,\mathrm{eff}} = (1 \pm \frac{|\Delta\omega|}{2\omega_p}) B_2 = \frac{\omega_{n0}}{\omega_p} B_2 , \qquad (3.1.7)$$

where the plus and minus signs correspond to the high- and low-frequency ENDOR lines, respectively, and ω_p is the free proton frequency. However, since the rf power by a search coil having an ω- dependent induced voltage,

$$V = -\frac{dF}{dt}\ \omega_{n0} B_2 , \qquad (3.1.8)$$

---

8 J. H. Freed, D. S. Leniart, and J. S. Hyde, *J. Chem. Phys.*, **47**, 2762 (1967).

9 D. H. Whiffen, *Mol. Phys.*, **10**, 595 (1966).

we need not make any correction for this effect in the present work.

Fig. 3.5 shows the rf-power dependence of the high frequency ENDOR lines measured for different protons at - 80 ℃, using the value of the mw power indicated by arrows in Figs. 3.3 and 3.4. Fig. 3.6, which shows a reciprocal plot of Fig. 3.5 indicates that the data fall well along straight

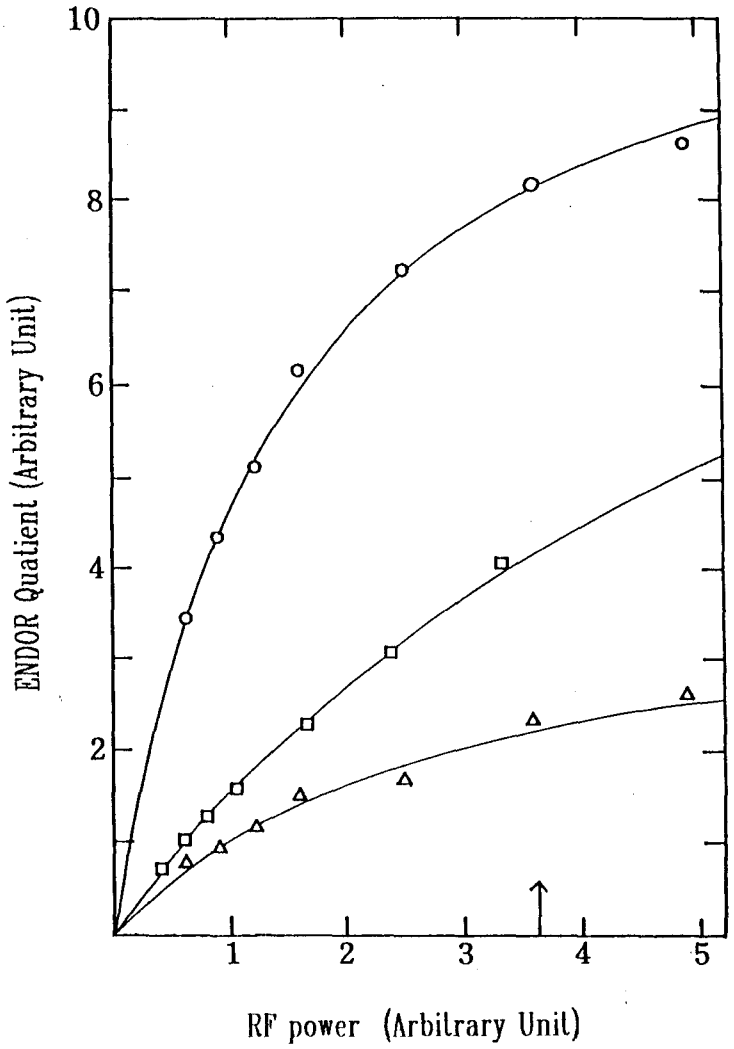

Fig. 3.5 ENDOR quotient as a function of rf power. The arrow indicates the rf power used for measurements of Fig. 3.3 and 3.4 .

lines,[10] as easily understood by

$$E_{\infty} = E_{\infty\infty} \frac{\gamma_n B_2 T_{2e}}{1 + T_{2n}^2 (\omega_{n0} - \omega_n)^2 + \gamma_n^2 B_2^2 T_{1n}(\mathrm{ON})\, T_{2n}} . \qquad (3.1.9)$$

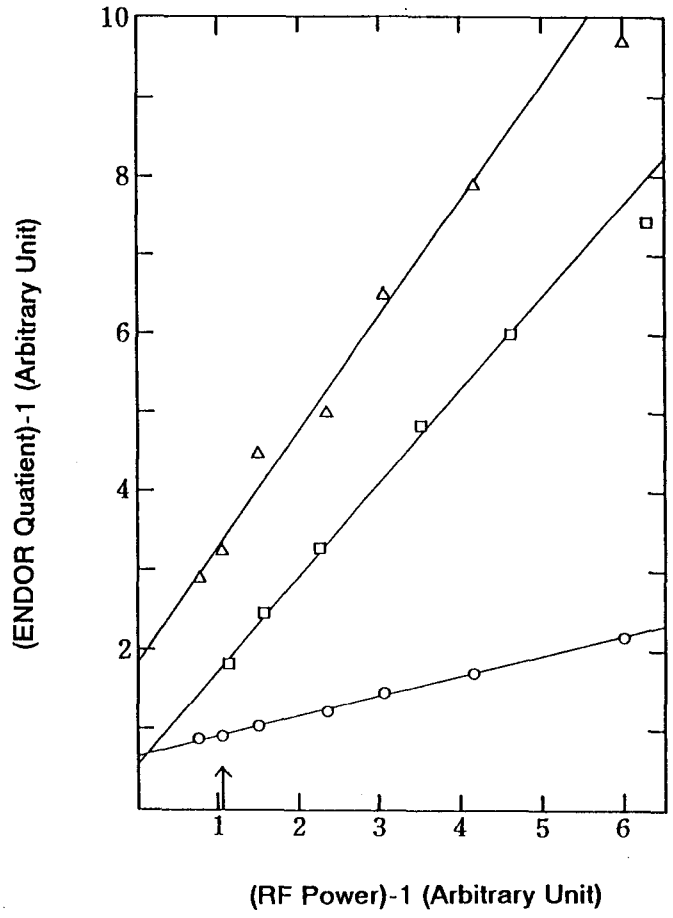

Fig. 3.6 Reciprocal of the ENDOR quotient as a function of the reciprocal of the rf power. The triangle are for *t*-butyl protons, circles for ring protons, and squares for a methylidyne proton.

---

[10] The plot for *t*- butyl protons appears to be curved downward. This fact is explained by the theory in Chapter 2 for a multi-level system, i. e., a plot of y^{-1} vs. x^{-1} in Eq. (2.3.100) there is, strictly saying, curve downward.

with the longitudinal relaxation time of a proton,

$$T_{1n} = \frac{1}{2W_n}\frac{C}{A} \tag{3.1.10}$$

where

$$A = (1 + b + b')\{2b + (b_{x1} + b_{x2})(1 + b) + 2b_{x1}b_{x2}\}, \tag{3.1.11}$$

$$C = (1 + b_{x1})(1 + b_{x2}) + (2 + b_{x1} + b_{x2})(b + \frac{b'}{2}). \tag{3.1.12}$$

Also, the above equation indicates that the line width of the ENDOR enhancement increases as the rf power increases, which agrees with what is found experimentally. On the other hand, it is found that this line width decreases with temperature decrease. This is qualitatively explained by the same equation, considering that the T_{2n} of a radical is mainly composed of W_e (See Eq. (2.3.147)).

3.1.5 Dependence on Temperature

The ENDOR enhancement is known to vary with temperature in a rather interesting fashion; it sharply increases to a maximum at a specific value of the ration of the viscosity to the temperature, $(\eta/T)_{opt}$, independent of the kind of solvent.[11] $(\eta/T)_{opt}$ increases as the size of the molecule decreases[12] and as the spin density on carbon atom to which an observing proton is bonded, decreases.[11,12] All this appears to be due to the fact that the fractional ENDOR enhancement is maximum at the temperature for which

---

11 Y. Kotake and K. Kuwata, *Bull. Chem. Soc. Jpn.*, **47**, 45 (1974)

12 K. Ishizu, M. Ohnishi, and H. Shikata, *Bull. Chem. Soc. Jpn.*, **50**, 76 (1977).

$b = W_n / W_e$ takes a certain value characteristic of the observed proton. Accordingly, from an analysis of the temperature dependence, it should be possible to obtain the value of b for different proton in a molecule or even information about its spin distribution. However, because an actual molecule contains several sets of equivalent protons, it is preferable for a quantitative discussion to use a theory for a multi-level system rather than the simple theory for a four-level system. Such a theory has been already developed in Chapter 2 Sec 2.3.6. It predicts that the ENDOR enhancement is proportional to the number of equivalent protons, if a sufficiently weak rf power is irradiated with $b \ll 1$ and the effect of incomplete hf separation can be neglected. This has sufficient value for use as an analytical tool such that its applicability should be examined experimentally over the whole temperature range used in ENDOR measurements.

For the above reasons, the ENDOR quotients for different protons in galvinoxyl were measured at temperatures from - 20 to - 95 ℃, by varying the rf power at five points for each temperature. Such measurements and a comparison of the results with theory requires careful specification of both the mw and rf powers. It was shown in Fig. 3.4 that the slope divided by the intercept for a methylidyne proton is identical to that for ring protons. This means the ratio of the ENDOR quotient for both protons at any mw power is identical to that at infinite mw power. The mw power employed in this experiment corresponds to the the maximum EPR intensity. Also, the rf power can be specified if the reciprocals of the slope and the intercept are determined from a similar plot shown in Fig. 3.5, because they correspond to the ENDOR quotients at infinitesimal and infinite rf powers, $E_{,0}^{exp}$ and $E_{,\infty}^{exp}$, respectively. $E_{,0}^{exp}$ and $E_{,\infty}^{exp}$, thus determined are shown in Figs. 3.7 and 3.8 as a function of η / T. These are analyzed using the

following procedure.

a) Simulation

According to the theory of Chapter 2 , Sec 2. 3.6, the fractional ENDOR enhancement at infinitesimal and infinite mw power is represented by

$$E_{,\infty}^{(u)} = r_H \sum_{J_u} \frac{D_{J_u}}{D_u} \frac{2 f_{J_u} b_u}{(1 + f_{J_u} b_u)(2 + f_{J_u} b_u)} \Big/ w(\mathrm{OFF}) \ . \quad (3.1.13)$$

For infinitesimal rf power irradiated on even number of equivalent protons ($\rho_n \ll 1$):

$$E_{,0}^{(u)} = r_H \sum_{J_u} \frac{D_{J_u}}{D_u} \frac{2 f_{J_u} \rho_n^{(u)}}{(2 + f_{J_u} b_u)^2} \Big/ w(\mathrm{OFF}) \ . \quad (3.1.14)$$

with similar equations for odd number of equivalent protons, where

$$w(\mathrm{OFF}) = 1 + \sum_{u} \sum_{J_u} \frac{D_{J_u}}{D_u} \frac{2 f_{J_u} b_u^2}{(2 + f_{J_u} b_u) b_u}$$

$$+ \sum_{u'} \sum_{J_{u'}} \frac{D_{J_{u'}}}{D_{u'}} \left\{ \frac{(f_{J_{u'}} - 1) b_{u'}^2}{\{2 + (f_{J_{u'}} - 1) b_{u'}\} b_{u'}} + \frac{f_{J_{u'}} b_{u'}^2}{(2 + f_{J_{u'}} b_{u'}) b_{u'}} \right\} , \quad (3.1.15)$$

with

$$r_H = \frac{(1 - \alpha)\rho_e}{1 + (1 + \alpha)\rho_e} \tag{3.1.16}$$

The transition probabilities in these equations have been formulated by Freed and Fraenkel[14] and by Freed.[15] Accordingly, if we have information about the g tensor, hf tensor and other molecular parameters of this radical, we can calculate, in principle, these values and thus the fractional ENDOR enhancement. Atherton and Day[16] have performed such an estimation for a methylidyne proton in galvinoxyl. However, this involves considerable ambiguities at the present stage. For instance, the rotational correlation time of a molecule, τ_R, is expressed by the extended Debye relationship as

$$\tau_R = \frac{4\pi\kappa r^3 \eta}{3kT} \tag{3.1.17}$$

The hydrostatic radius, r, and a constant, κ, are both dependent on the molecular structure of the radical and the solvent, and consequently, involve unavoidable ambiguities.

For this reason, here, only the η/T dependence of each transition probability is assigned under the following assumptions in an attempt to examine how the fractional ENDOR enhancement varies with temperature. A moderately slow tumbling molecular motion is assumed so that the following conditions are satisfied:

$$\omega_{e0}^2 \tau_R^2 >> 1, \ \omega_{n0}^2 \tau_R^2 << 1. \tag{3.1.18}$$

---

14 J. H. Freed and G. K. Fraenkel, *J. Chem. Phys.*, **39**, 326 (1963).

15 J. H. Freed, *J. Chem. Phys.*, **43**, 2312 (1965).

16 N. M. Atherton and B. Day, *Mol. Phys.*, **27**, 145 (1974).

For W_e, we neglect the contribution from the END interaction, as well as the spin rotational interaction, and thus it is assumed to be independent of the nuclear spin quantum numbers. Then, denoting the spectral density by $j(\omega)$, the η/T dependence of the transition probabilities can be written as

$$W_e \sim 2j_{G_2}(\omega_{e0})B_0^2 \sim \tau_R^{-1} \sim (\eta/T)^{-1} \tag{3.1.19}$$

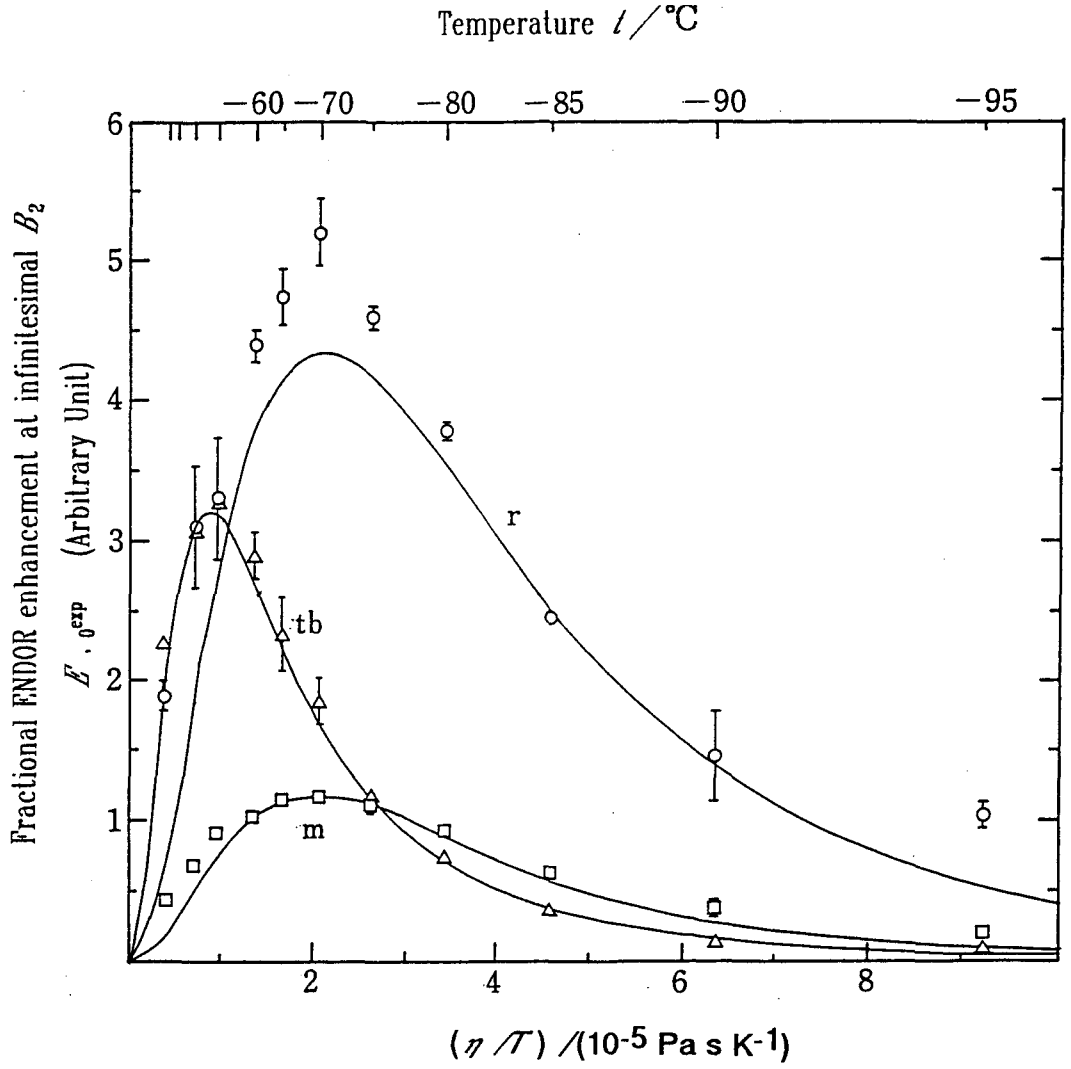

Fig. 3.7 $E_0{}^{exp}$ as a function of η/T, □ for a methylidyne proton, ○ for ring protons, and △ for *t*-butyl protons. The vertical lines indicate the probable error, as determined by the least-squares method. The solid lines are theoretical results.

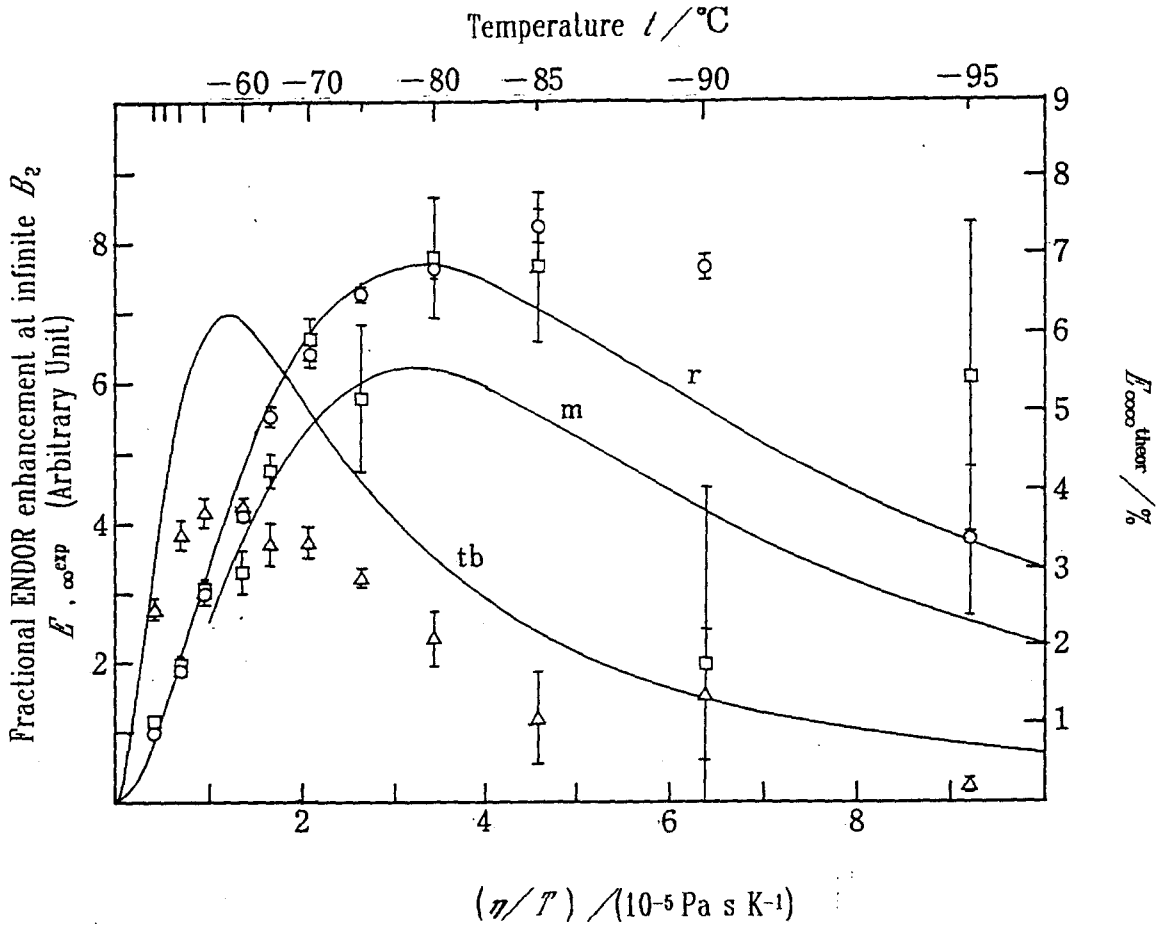

Fig. 3.8 $E_{,\infty}^{\exp}$ as a function of η/T, □ for a methylidyne proton, ○ for ring protons, and △ for *t*-butyl protons. The vertical lines indicate the probable error, as determined by the least-squares method. The solid lines are theoretical results.

and

$$W_n(u) \sim j_D^{(u)}(0) \sim \tau_R \sim \eta/T, \qquad (3.1.20)$$

so that

$$b_u \sim \frac{j_D^{(u)}(0)}{4j_{G_2}(\omega_{e0})} \sim \tau_R^2 \sim (\eta/T)^2 \qquad (3.1.21)$$

Also, the η/T dependence of T_{2n} is derived from

$$\frac{1}{T_{2n}(J_u)} = W_e\{1 + (2f_{J_u} + \frac{1}{3})b_u\} \qquad (3.1.22)$$

We assume p_e and T_{2e} to have to have constant value of 1/2 and 1.2 ms, respectively, independent of the temperature. (The choice of the latter value is discussed below.) If we choose given value of b_m, b_r, and b_{tb} at any temperature and apply these equations to Eqs. (3.1.12) - (3.1.14) the relative value of $E_{,0}$ for each proton in galvinoxyl are readily evaluated for all temperatures. Thus, the value of b_m, b_r, and b_{tb} are determined in such a way that the experimental and theoretical T_{opt} for $E_{,0}$ are in complete agreement, since the T_{opt} for $E_{,0}^{exp}$ are known precisely for each proton. Then, using the value of b thus determined, the values of $E_{,\infty}$ are calculated for each proton from Eqs.(3.1.11) and (3.1.13). The results are shown by solid line in Figs. 3.7 and 3.8. In Fig. 3.7, the values of $E_{,0}$ are normalized to that of E_0^{exp} for a methylidyne proton at the optimum temperature for this proton.

b) Methylidyne and Ring Protons

Because the determination of E_0^{exp} involves much smaller errors than that of E_∞^{exp}, the T_{opt} in Fig. 3.7 are unambiguously obtained to be - 70 ℃, - 70 ℃ and - 50 ℃ for the methylidyne, ring and *t*-butyl protons, respectively. On the other hand, these temperatures are not clear in Fig. 3.7. However,

repeated experiments indicate the T_{opt} to be about - 55 ℃ for *t*-butyl protons, - 80 - - 85 ℃ for the methylidyne and ring protons. Thus, E_0^{exp} has a maximum at a value of η/T of about one-half of that for E_∞^{exp}. In addition, E_0^{exp} decreases more rapidly than does E_∞^{exp} for temperatures below the T_{opt}. The theoretical curves can describe these features well. However, at very low temperatures, the theoretical curves tend to be below the experimental points in both figures, as was more evidently confirmed from repeated experiments. This is believed to arise from the $b_u << 1$ assumption which is invalid at these temperatures. In Eqs. (3.1.11) - (3.1.13), the relaxation pathways for the END terms of protons other than that observed contribute only to the denominator, so that the fractional ENDOR enhancement tends to be underestimated when $b_u \geqq 1$.

Regarding the relative intensity, $E_{,0}^{exp}$ for the methylidyne proton in Fig. 3.8 is about four times smaller than that for the ring protons. This is more clearly indicated in Fig. 3.10 in which the ratio of the values of $E_{,0}$ for the ring and *t*-butyl protons to that for methylidyne proton are plotted against η/T. It is encouraging that the experimental and theoretical values of $E_{,0}$ for the methylidyne proton and ring protons are approximately proportional to the number of equivalent protons, 1 and 4, even at temperatures for which the condition, $b_u < 1$, is not necessarily valid. On the other hand, In Fig. 3.7, the $E_{,0}^{exp}$ for a methylidyne proton agrees with that for ring protons (see also Fig. 3.6), whereas the theoretical counterparts at optimum temperatures at - 79 ℃ ($b_m = 0.84$ and $b_r = 0.29$), are 5.6 and 6.9 % for methylidyne and ring protons, respectively, with a ratio of 1.26. The quantitative justification of these values is left until absolute measurements of fractional ENDOR enhancement are performed. However, it should be noted that the calculated values are much smaller than the value, 12.5 %, expected from the simple

theory for a four-level system.

It is worthwhile to discuss the correlation of the values of b estimated from Fig. 3.8 with the spin distribution in galvinoxyl. The value of b obtained at - 70 ℃ (η/T= 2.05 × 10^{-5} Pa s K^{-1}) are b_m = 0.32 and b_r = 0.11 with b_m/b_r = 2.9. Luckhurst[17] has studied in detail the structure and the spin distribution of galvinoxyl, and has found ρ_m = - 0.0748 and ρ_r = - 0.0448. It is considered that $W_n(u)$ is proportional to the square of the spin density on the carbon atom to which the u-th proton is bonded.[11,18] Then the above ratio of $b$values should be 2.79. The good agreement between both values shows close correlation between the spin density and the ENDOR relaxation. Also, the agreement seen at high temperatures between $E'_{\infty}{}^{exp}$ values for methylidyne and ring protons in Fig. 3.9 leads to a ratio in the neighborhood of 2, using Eq. (2.3.157).

c) t-butyl Proton - the Effect of Incomplete Hf Separation

Now the ENDOR quotient for *t*butyl protons will be considered. The experimental results show two peculiar features;

(1) the high optimum temperature, as seen in both Figs. 3.7 and 3.8, in spite of the fact that proton with a smaller END term should have a lower optimum temperature, and

(2) the much smaller ratio of $E'_{0}{}^{exp}$ for this proton to that for methylidyne proton than would be expected from the number of equivalent protons, 1 : 36 (see Fig. 3.9).

Such a high optimum temperature for this proton is also found for 2,4,6-*tri-t*-butylphenoxyl,6 2,5 -*di-t*- butyl - *p* -benzosemiquinone[11] and *m,m,m',m'*-

---

17 G. R. Luckhurst, *Mol. Phys.*, **11**, 205 (1966).

18 J. H. Freed, *J. Chem. Phys.*, **71**, 38 (1967).

tetra-t-butylbiphenyl[12] and appears to be characteristic of *t*-butyl protons. Allendoerfer and Maki[6] have suggested that this is attributable to the effect of incomplete hyperfine separation, mentioned below. Considering only the secular terms for the same assumption under which Eq. (3.1.17) is based, T_{2e} may decrease with temperature as follows

$$\frac{1}{T_{2e}} \sim \frac{8}{3} j_{G_2}(0) B_0^2 \sim \tau_R \sim \frac{\eta}{T}, \tag{3.1.23}$$

so that this effect is more prominent at lower temperature and thus results in a higher optimum temperature.

However, simulation shows that this effect requires a T_{2e} as short as 10 ns at - 50 ℃ in order to reproduce such a high optimum temperature, but then the ENDOR enhancement will become negligibly small by this effect. In addition the apparent EPR line width for galvinoxyl was found to decrease with temperature down to - 20 ℃, is constant as a whole from - 20 to - 70 ℃, and increases rapidly at lower temperatures. Perhaps, nonsecular and pseud-secular terms, as well as the contribution from the spin rotational interaction, may compete with secular terms in Eq. (3.2.10) at high temperature, as the result, T_{2e} not so much varies with temperature.

It is believed that the high optimum temperature is attributable to the large average total nuclear-spin quantum number of the *t*-butyl protons. Let us assume a crude 4-level system for *t*-butyl protons whose relaxation pathway involves only W e and $\langle W_n^{(u)} \rangle$, the average nuclear-spin quantum number, which is given by

$$\langle W_n^{(u)} \rangle = \sum_{J_u} \frac{D_{J_u}}{D_u} J_u(J_u + 1) W_n^{(u)} = \frac{1}{2} n_u W_n^{(u)}. \tag{3.1.24}$$

Then the fractional ENDOR enhancement is optimized when

$$\frac{1}{2} n_u b_u = 1 \qquad (3.1.25)$$

Therefore, the fractional ENDOR enhancement for a proton species with many equivalent protons has a high optimum temperature.

The much smaller value of E_0^{exp} for *t*-butyl protons than for other protons evidently results from the effect of incomplete hf separation. However, the choice of the value of T_{2e} involves ambiguities, because inhomogeneous broadening unfortunately prevent an estimation of T_{2e} from the unsaturated EPR linewidth. The T_{1e} of galvinoxyl in *s*-butylbenzene, determined by Huisjen and Hyde[19] from saturation recovery, has a value in the range 1 - 10 ms at - 30 ℃. If the extreme narrowing condition is satisfied at this temperature, T_{2e} may also be of the same order of magnitude. Here, T_{2e} was taken as a constant with a value 1.2 ms, from consideration of the behavior of the EPR linewidth, mentioned above. Then, the optimization process for *t*-butyl protons gave $b_{tb} = 0.19$ at - 70 ℃, whereas $b_{tb} = 1/18$ at - 55 ℃, or converted to $b_{tb} = 0.19$ at - 70 ℃, from Eq. (3.2.12). It is felt that these values of b_{tb} are rather large compared with those for other protons. A possible explanation may be the closeness of the location of *t*-butyl protons to oxygen atom which has large spin density, resulting in large END term.

The theoretical solid curves, calculated from Eqs. (3.1.11) - (3.1.14), are close the experimental curves in Figs. 3.7 and 3.8. Also, Fig. 3.9 shows that the ratio of E_0^{exp} for *t*-butyl protons to that for a methylidyne proton decreases monotonically with temperature, in contrast to ring protons which

---

19 M. Huisjen and J. S. Hyde, *J. Chem. Phys.*, **60**, 1682 (1974).

have almost constant value 4. Such a feature is again described by the theoretical solid lines. It is to be noted that the dotted line, calculated from Eq. (3.1.12) in which the first factor is omitted, or the effect of incomplete hyperfine separation is neglected, has a value much smaller than 36, except at extremely high temperatures. The above discussion for *t*-butyl protons should not be taken too seriously, since the present lack of information about the internal motion of the *t*-butyl groups prevents further consideration, such as of the isotopic hyperfine modulation. Nevertheless, it

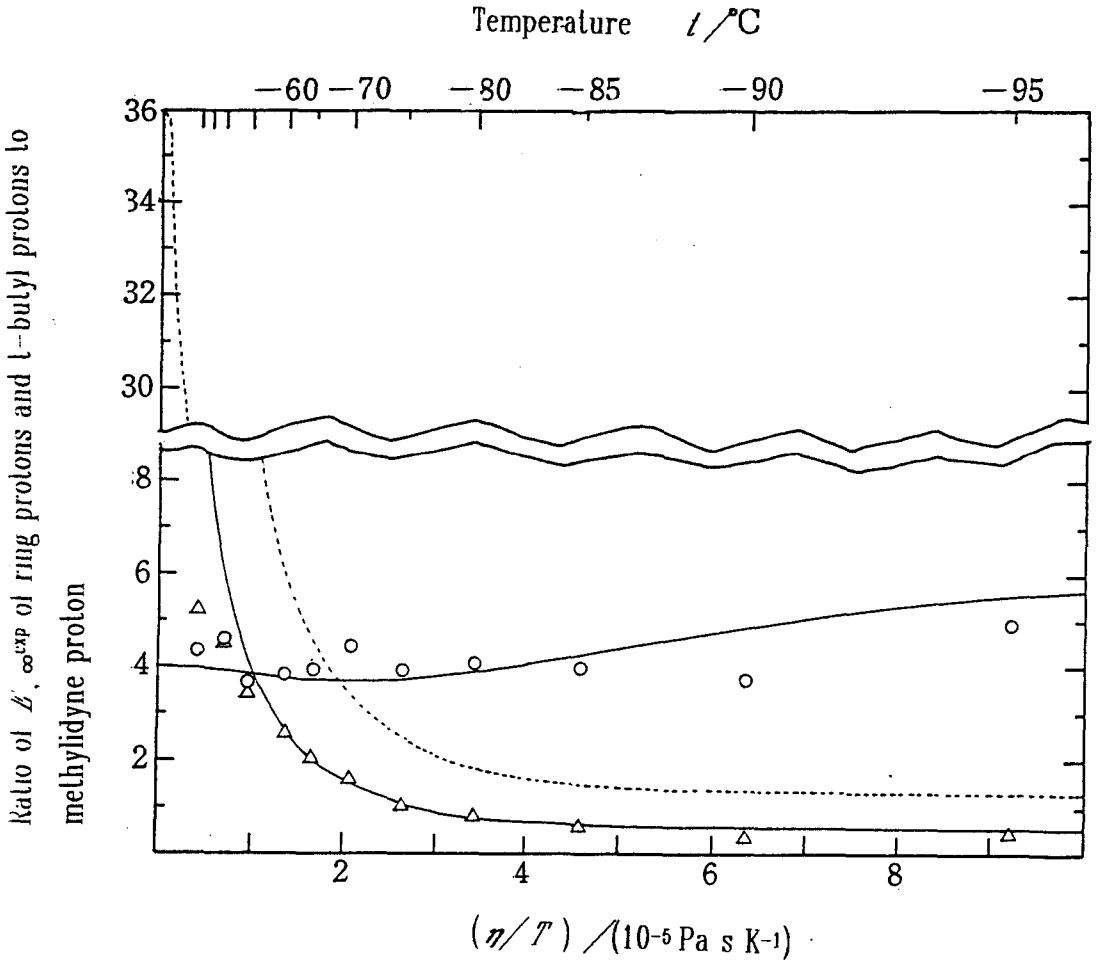

Fig 3.9 Ratio of $E'_0{}^{exp}$ values for *t*-butyl protons (△) and ring protons (○) to $E'_0{}^{exp}$ for a methylidyne proton as a function of η/T. The solid lines are theoretical results.

is felt that the essential features of the ENDOR quotient for *t*-butyl protons can be explained by the effect of incomplete hyperfine separation and the large average multiplicity for this proton discussed above.

In conclusion, it may be said that the theory developed in the present work describes fairly well the ENDOR relaxation of galvinoxyl.

3.2 ELDOR Relaxation of Galvinoxyl

3.2.1 Introduction

In this section, we report the results of application of ELDOR spectroscopy to the study of the relaxation mechanism of an organic radical in liquid phase. The radical used in the study is the galvinoxyl in toluene solution, which has been studied, in detail, by the ENDOR method as already described in Section **3.1**. Also, we have seen in Chapter 2 that the phenomenological theory based on the spin population number method can equally treat ELDOR reduction as well as ENDOR enhancement satisfactorily. We have seen that both ENDOR and ELDOR spectroscopies measure the change in the EPR intensity resulting from the partial short-circuit of the nuclear- and electron spin relaxation pathways, respectively. ENDOR enhancement and ELDOR reduction are even naturally formulated in terms of similar kinds of relaxation probabilities, but they are expressed in quite different fashions. In a sense, ENDOR- and ELDOR spectroscopies may be said to have complimentary role for the study of the double resonance relaxations. Thus it is only obvious that the combined usage of

the both methods to *a same radical* will allow us to look over relaxational behavior of the radical stereo-graphically, and more abundant and more accurate information about its relaxation probabilities will be expected. Nevertheless, few studies along the scheme on this line are reported in literatures. This is just one motive force of the present study.

From the viewpoint of the relaxation study, ELDOR spectroscopy has some merits compared with ENDOR spectroscopy.

The first is of experimental. The fractional ELDOR reduction of a liquid phase radical is much larger than the fractional ENDOR enhancement. It often comes up more than fifty percent reduction. Therefore we can accurately measure the absolute value of the fractional ELDOR reduction itself from the field-swept EPR spectra of the observing mode under pumping mode mw irradiation, which enables to compare the absolute value of the experimental fractional ELDOR reduction with its theoretical value. By contrast, ENDOR enhancement is usually measured indifferent to its EPR intensity, because the fractional ENDOR enhancement is typically only a several percent.[20] This value is too small for comparison of absolute experimental value of fractional ENDOR enhancement with the theoretical one.

The second is of theoretical. In ENDOR, one rf field corresponding to a proton species results in changes of all of relaxation pathways by ρ_n's among multiplet spin levels corresponding to that species. Such situation makes multi-level analysis more suitable for ENDOR, and it is compared with ELDOR, in which the pumping mw field almost influences only population on a four spin-level. Perhaps, such suitability may be the same for taking into consideration of Heisenberg spin exchange effect.

---

[20] J. S. Hyde, *J. Chem Phys.*, **43**, 1806 (1965).

Furthermore, as long as for a four-level system, the theory in Chapter 2 as well as the relaxation matrix theory derives the fractional ELDOR reduction in much simpler form than the fractional ENDOR enhancement. This enables more easier analysis of the experimental data: The fractional ELDOR reduction of this system, when the END and the HE terms are the only significant relaxation pathways, is given by

$$R_{0\infty} = \frac{b + b'}{b + b' + 2}, \tag{3.2.1}$$

as the limiting formula with very small observing mode mw and infinite magnitude of pumping mode mw. This is compared with complex form of Eq. (2.3.95) of the fractional ENDOR enhancement in the same condition. Simpleness of the former will allow more simple analysis.

On the other hand, experimental difficulty arises in ELDOR spectroscopy, coming from the fact that the pumping mode and the observing mode alternating fields are both mw field and that ELDOR requires very strong power of pumping mode mw, which must be, at the same time, completely separated from the observing mode mw. This is compared to ENDOR in which two different kinds of field, mw and rf are irradiated. At least 3 MHz of the magnitude of hfs should be required for completely separated ELDOR measurement. ENDOR spectroscopy has no such limitation.

The galvinoxyl radical is very suitable for the ELDOR study. It has one methylidyne proton with hfs constant of 15.55 MHz, four ring protons with 3.89 MHz, and thirty-six *t*- butyl protons with 0.12 MHz. Therefore we have completely separated mw frequencies for ELDOR for the doublet by methylidyne proton. Also, the much larger hfs of one methylidyne proton than others allows approximately a four-level system as the basis of

theoretical analysis of ELDOR reduction of this radical.

The ELDOR reduction of galvinoxyl has already been reported by Hyde *et al*[21]. However their results seem to be of preliminary nature, and no detailed measurements and quantitative analysis were made in their study. In the present study, much more detailed measurements were made for the ELDOR reduction of galvinoxyl, varying temperature from 10 ℃ to - 85 ℃, with concentration from 2.6×10^{-3} mol l^{-1} to 8.1×10^{-5} mol l^{-1}, and the theoretical analysis was made using theory for a four-level spin system.

3.2.2 Experimental

The purity of the galvinoxyl radical synthesized in this laboratory was determined to be 92 % from the measurement of the static magnetic susceptibility. The toluene solution of this radical was degassed in a quartz tube by a usual method. The radical concentration was controlled by repeating the twice dilution method of the original sample with a known concentration.

The ELDOR reduction was observed using a Varian E-800 ELDOR unit with a bimodal cavity in which TE_{102} observing- and pumping mode microwaves are rectangularly distributed each other. The unit is attached to a 100 kHz field modulated EPR spectrometer of home made. The pumping krystron in the apparatus can provide about 900 mW of the mw power. The field swept ELDOR spectra were observed as follows: The unsaturated EPR spectra were observed with the observing mode mw of 9.13 GHz as shown in Fig. 3.10 (b). Then the pumping mode mw of frequency higher by 16.59 MHz, which corresponds to the approximate hfs constant of the

---

[21] J. S. Hyde and J. H. Freed, *J. Chem Phys.*, **48**, 4211 (1968).

methylidyne proton, was irradiated and the EPR spectra was again observed as shown in Fig. 3.11 (a). This frequency was selected as such giving maximum ELDOR reduction. Care was taken for saturation as well as overmodulation which is known to influence critically to ELDOR reduction.[21] From the intensity of the central peak of the high-field side of the doublet, the reduction factor was determined by

$$R = \frac{I(\mathrm{OFF}) - I(\mathrm{ON})}{I(\mathrm{OFF})}, \qquad (3.2.2)$$

where ON denotes the pumping mode mw irradiated and Off denotes it is negligibly small.

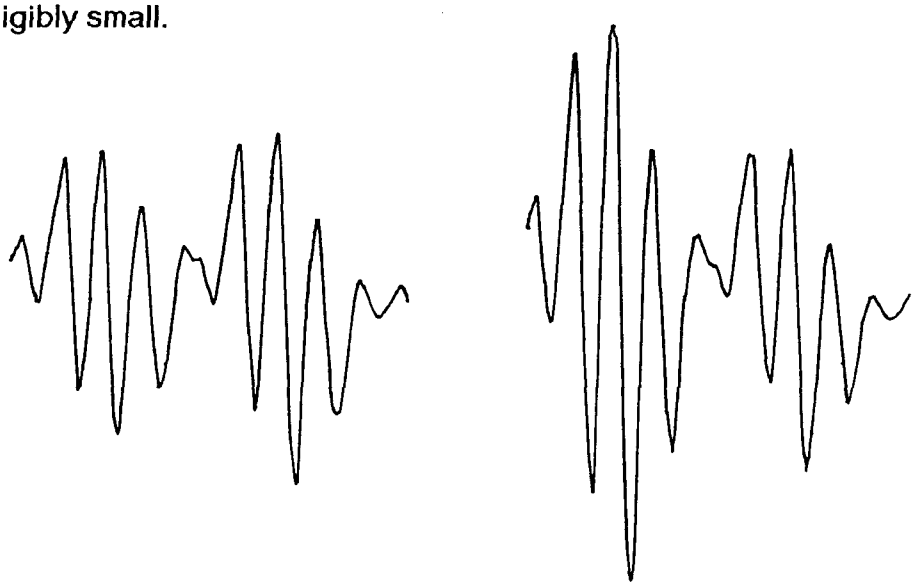

a) b)

Fig. 3.10 The spectra of galvinoxyl when the pumping mode mw is irradiated (a), with the original EPR spectra of galvinoxyl (b), at - 95 ℃. The low field side of the doublet in (a) is reduced by the ELDOR effect. (High field side is broadened in both figures because of viciousness of the solvent at low temperature.)

3.2.3 Results and Discussion

(a) Dependence on Temperature

Fig. 3.11 shows the dependence of the ELDOR reduction on pumping mode mw power, measured at temperatures from - 90 ℃ to 10 ℃. The plot

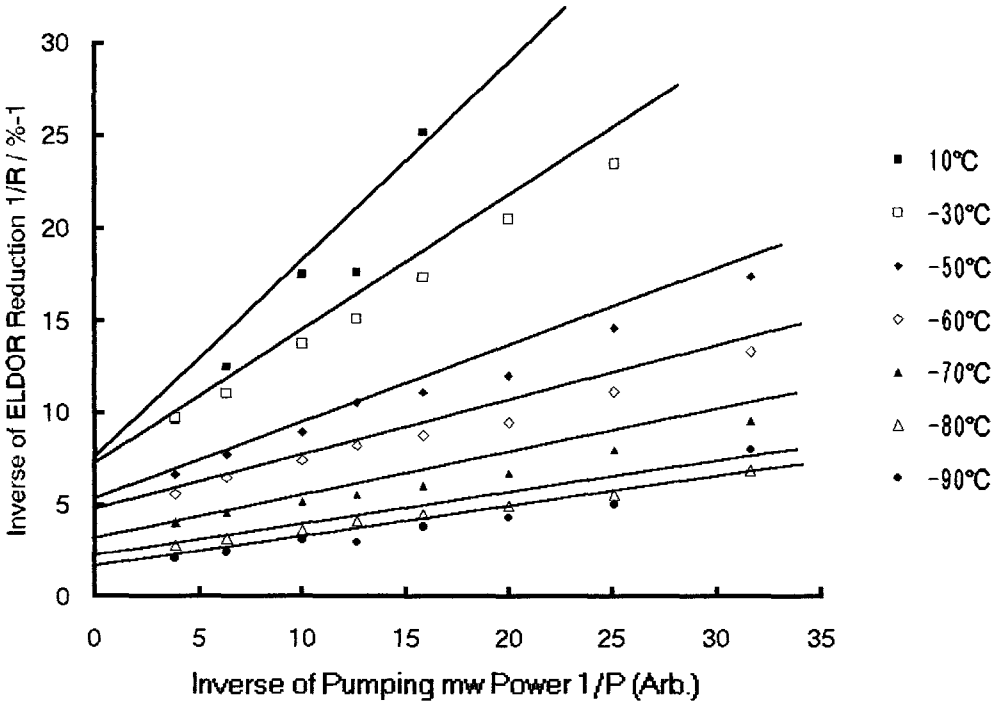

Fig. 3.11 Dependence of the fractional ELDOR reduction at different temperatures on pumping mode mw powers. The concentration is 3.3×10^{-4} M.

of the reciprocal of the fractional ELDOR reduction against the reciprocal of the pumping mode mw power gives good straight lines. The fractional ELDOR reduction at infinitesimal observing mw power is given from Eq. (2.3.140) as the formula in which cross relaxation terms are omitted reasonably,

$$R_0 = \frac{(b + b')\rho_p}{2(b + b' + 1) + (b + b' + 2)\rho_p}, \qquad (3.2.3)$$

where

$$\rho_p = \frac{1}{2}\gamma_e^2 B_p^2 T_{2e} \frac{1}{1 + T_{2e}^2 (\omega_p - \omega_{p0})^2} . \qquad (2.3.134)$$

Therefore the reciprocal of the intercept corresponds to the ELDOR reduction at infinite pumping power irradiated, $R_{0\infty}^{exp}$, which is formulated

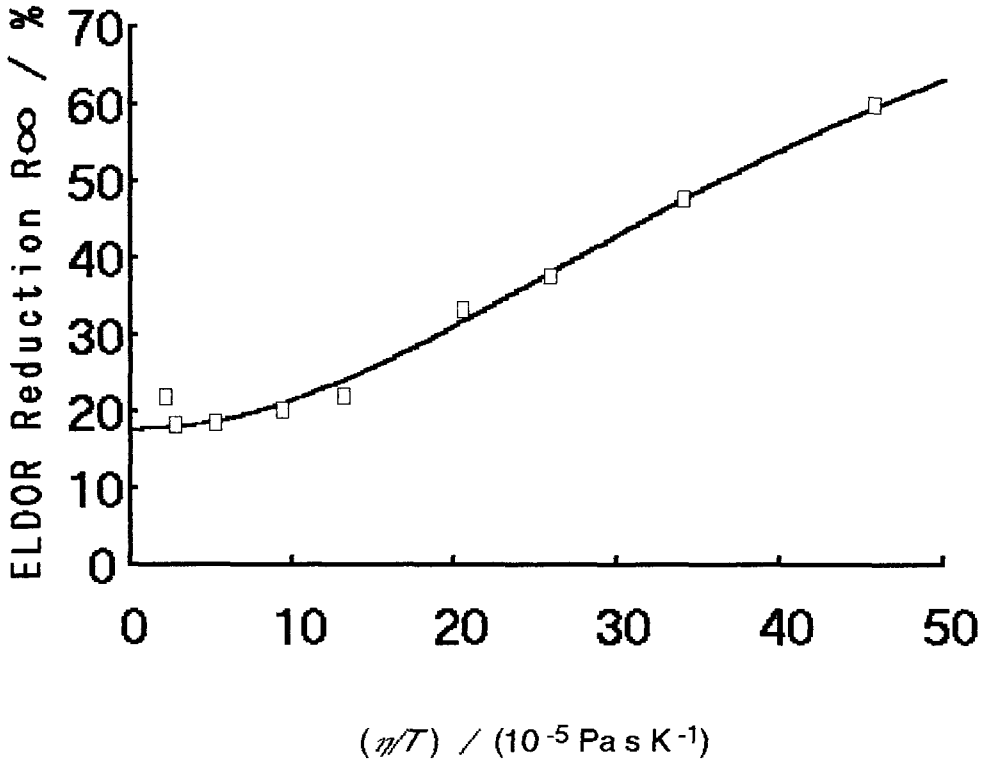

Fig. 3.12 the fractional ELDOR reduction at infinite pumping mw power plotted against (η/T).

by Eq. (3.2.1) . The results, thus obtained, are plotted in Fig. 3.12 as a function of η/T.

If we naturally assume a moderately slow tumbling molecular motion, so that the following conditions are satisfied:

$$\omega_{e0}^2 \tau_R^2 >> 1, \ \omega_{n0}^2 \tau_R^2 << 1, \tag{3.1.18}$$

then the following temperature dependence will be expected for electron

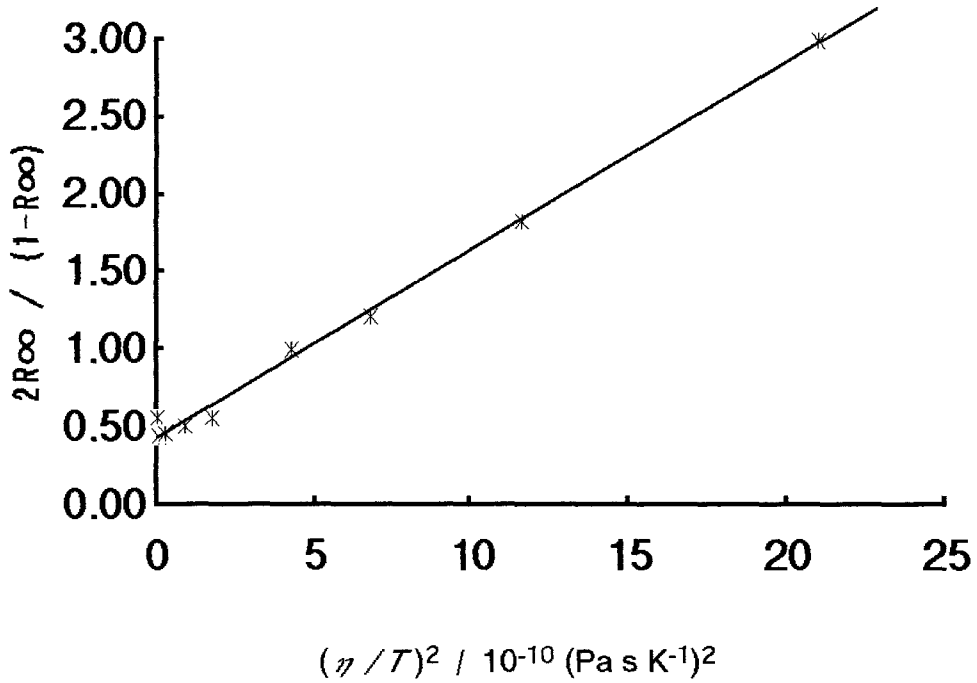

Fig. 3.13 Dependence of $R_{0\infty}^{exp}$ as a function of temperature. The plot of $2R_{0,\infty} / (1 - R_{0,\infty})$ against $(\eta/T)^2$.

spin transition, nuclear spin transition, and Heisenberg spin exchange, respectively:

$$\begin{aligned} W_e &\sim \tau_R^{-1} \sim (\eta/T)^{-1}, \\ W_n &\sim \tau_R \sim \eta/T, \\ \omega_{HE} &\sim \tau_R^{-1} \sim (\eta/T)^{-1}. \end{aligned} \tag{3.2.4}$$

Thus

$$b = W_n / W_e \sim (\eta / T)^2,$$
$$b' = \omega_{HE} / W_e \sim \text{const.} \qquad (3.2.5)$$

Therefore from Eq. (3.2.1), the plot of $2 f_{0,\infty} / (1 - f_{0,\infty})$ against $(\eta / T)^2$ will become a straight line. Indeed Fig. 3.13 shows linearity for this plot. Figs. 3.12 and 3.13 indicates that at very high temperature, the END term is not so responsible and the Heisenberg spin exchange effect is the principal mechanism for ELDOR reduction, whereas at low temperatures smaller than - 50 ℃ the END terms play important role. We obtain from the plot,

$$b' = 0.42$$
$$b = 0.52 \text{ at } -70 \text{ ℃}. \qquad (2.3.6)$$

The curve on Fig. 3.12 is the calculated curve from such lineality. It matches nicely with the measured points.

b) Dependence on Concentration

To examine dependence of ELDOR reduction on concentration, dependence of the fractional ELDOR reduction on pumping mode mw power was measured at - 70 ℃, varying the concentration from 2.6×10^{-3} to 8.1×10^{-4} M. From reciprocal plots similar to Fig. 3.11, the fractional ELDOR reduction at infinite pumping power was obtained as the function of concentration, as shown in Fig. 3.14. Since b' is simply proportional to concentration, similar analysis as Fig. 3.13 gives linear plot of Fig. 3.15. The value of b and b' obtaind from the plot are

$b = 4.7$,

$b' = 0.50$ at concentration, 3.3×10^{-4} M. (3.2.7)

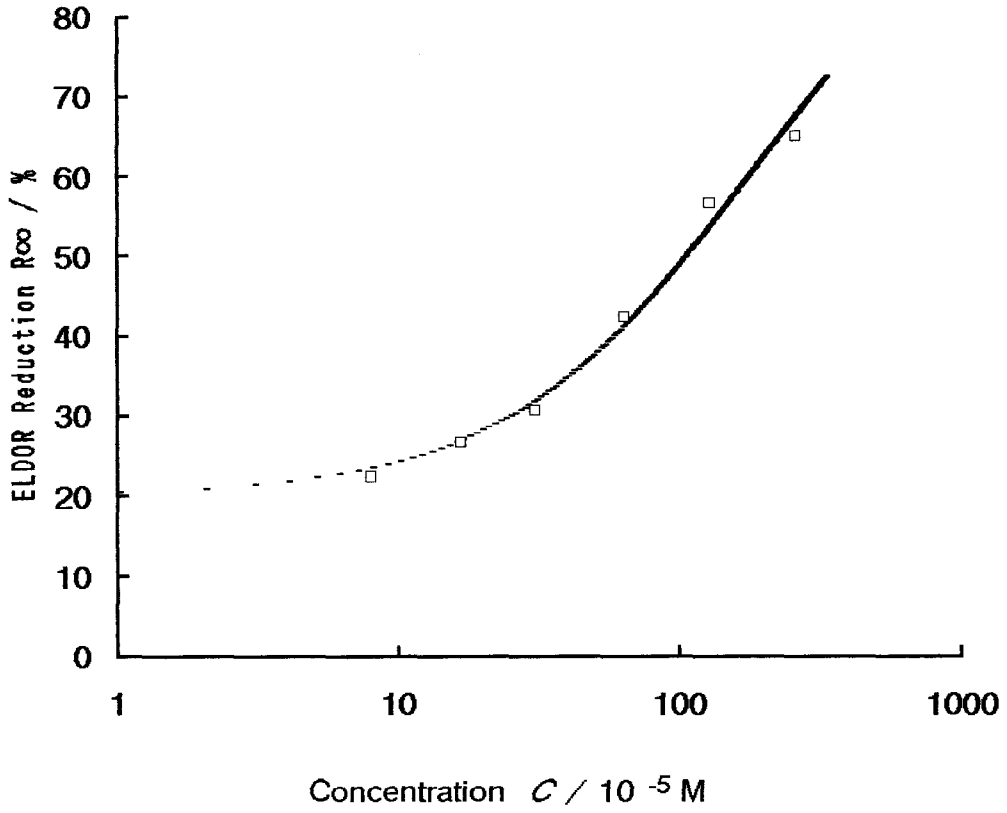

Fig. 3.14 Fractional ELDOR reduction measured at - 70 ℃ as a function of concentration.

The curve in Fig. 3.14 is again calculated from the lineality of Fig. 3.15, and the both figures indicate that Heisenberg exchange is not effective for ELDOR reduction at very low concentration, but rapidly become important as concentration increases. The good agreement of Eqs. (3.2.6) and (3.2.7) justifies the present analysis, and further suggests the moderate slow tumbling motion of the radical is suitable assumption in our temperatures and concentrations.

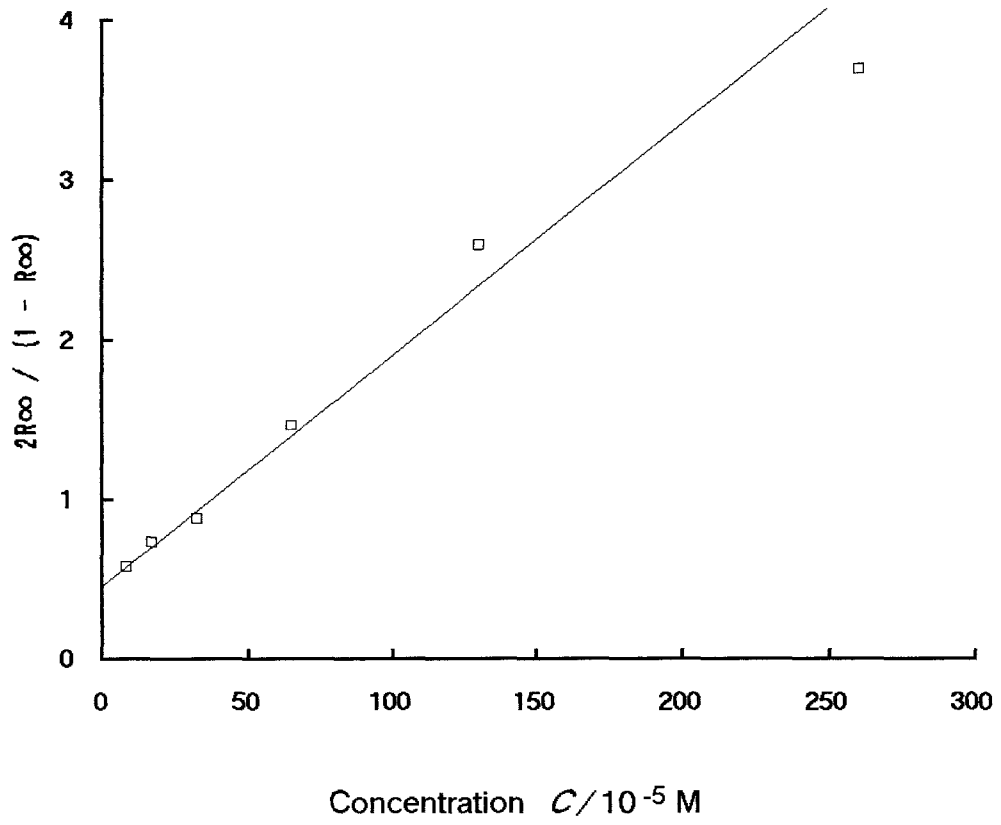

Fig 3.15 $2R_{0,\infty}/(1 - R_{0,\infty})$ as a function of concentration.

In ENDOR experiment we have estimated the value of b_m to be 0.32 at - 70 ℃. this value seems to be somewhat lower than those of Eq. (3.2.6) and (3.2.7). the dfference corresponds to the temperature descrepancy of about 4K, and whether such difference is meanful or not is the problem left in future. Also we have neglected the Heisenberg spin exchange effect in the analysis of the ENDOR quatient. This is left as an another problem to be solved.